Expression and Purification of Cytosolic Domains of Cyclic Nucleotide Gated Calcium Channel (CNGC19)

A Thesis

Submitted to

Indian Institute of Science Education and Research Pune

in partial fulfilment of the requirements for the

BS-MS Dual Degree Programme

by

Bhawana

Indian Institute of Science Education and Research Pune

Dr.Homi Bhabha Road,

Pashan, Pune 411008,India.

April, 2020

Supervisor

Dr. Jyothilakshmi Vadassery (NIPGR, Delhi)

TAC: Dr. Sagar Pandit (IISER Pune)

© Bhawana, 2020

All rights reserved.

CERTIFICATE

This is to certify that this dissertation entitled **‘‘Expression and Purification of Cytosolic Domains of Cyclic Nucleotide Gated Calcium Channel (CNGC19)”** towards the partial fulfilment of BS-MS dual degree programme at the Indian Institute of Science Education and Research, Pune represents the study/work carried out by Bhawana at NIPGR Delhi, under the supervision of Dr. Jyothilakshmi Vadassery, Scientist IV, NIPGR during the academic year of May 2019-March 2020.

Signature of the supervisor
Dr.Jyothilakshmi Vadassery
Staff Scientist IV
NIPGR, New Delhi 110067

Signature of the student
Bhawana
IISER Pune, 411008

Date : April 09,2020
Place: NIPGR, Delhi

DECLARATION

I hereby declare that the matter embodied in the report entitled **"Expression and Purification of Cytosolic Domains of Cyclic Nucleotide Gated Calcium Channel (CNGC19)"** are the results of the work carried out by me at National Institute of Plant Genome and Research, Delhi under the supervision of Dr. Jyothilakshmi Vadassery and the same has not been submitted elsewhere for any other degree.

Signature of the supervisor
Dr. Jyothilakshmi Vadassery
Staff Scientist IV
NIPGR, New Delhi 110067

Signature of the student
Bhawana
IISER Pune, 411008

Date : April 09,2020
Place: NIPGR, Delhi

This thesis is dedicated to my beloved parents and brother.

Thanks for always being there for me!

ACKNOWLEDGEMENT

The dissertation project carried out by me has been one of the greatest academic challenges of my life. I am deeply grateful to many individual and want to express my deep sense of thanks to all of them.

Firstly, I would like to express sincere gratitude to my supervisor Dr. Jyothilakshmi Vadassery for allowing me to work on this interesting project and cordial thanks for her extraordinarily support, patience, warm encouragements and motivation throughout the journey. I would like to express my deepest appreciation to Dr.Arockiasamy Arulandu (ICGEB) for allowing me to work in his lab and granting the best of the facilities available. I am thankful for receiving generous moral support and constant suggestions from him throughout the duration of my project.

I would also like to thank my TAC supervisor Dr. Sagar Pandit for his valuable teaching, and insightful support without which my dissertation would have been undoubtedly difficult. I will forever be thankful to my faculty members and all the seniors. Special thanks to my mentor Dr. D. Balasubramaniam for his unfailing cooperation and sharing his valuable time and knowledge which helped me sail through this project with ease. I would also like to thank Mahendra Varma for helping me in Bioinformatics. I owe my deepest gratitude to Dr. Pritha Kundu with whom I had the opportunity to share some projects.I am also thankful to Unais for helping me throughout the project.I would also like to thank Love for his constant support and coordination while carrying out my work.

I was fortunate to get the opportunity of working with such wonderful lab members at NIPGR and ICGEB. I thank all of them for providing me an excellent environment for helping me out. I also want to thank my family members for all their emotional and moral support, especially my parents for their constant motivation and being there for me at all times. Last but not least, I would like to thank my friends Nupur, Heena, Swati, Roshni, Shubhangi, Rani and Shikha for supporting me and making it possible by providing me with all the encouragement and affection.

TABLE OF CONTENTS

Contents

ABSTRACT

Plants have to deal with a plethora of abiotic and biotic stress during their life time. Insect herbivory is one such devastating biotic stress that affects the plant productivity worldwide. During evolution, plants have adapted to cope up with this stress condition by perceiving insect herbivory rapidly and activating defence response. Increase in cytosolic calcium level is a key defence response against herbivore attack. Various channels involved in exchange of calcium ions across cell membrane include Cyclic nucleotide gated channels (CNGCs), Glutamate like receptors (GLRs) and two-pore channels (TPCs). CNGCs are essential component of plant defence against insect attack. In Arabidopsis, CNGC19 was identified as the highly expressed upon Spodoptera herbivory. Functional characterisation of CNGC19 reveals that CNGC19 plays a key functional role in defence signalling against Spodoptera. However, the molecular mechanism of calcium flux through CNGC19 remains poorly understood mainly due to lack of three-dimensional structure and biochemical-biophysical characterization. The aim of this project is to overexpress, purify the cytosolic domains of CNGC19 and use them to determine the structure of AtCNGC19. This would help in providing broader view to decipher the physiological role of CNGC19 and it would also help in understanding the molecular basis of calcium signalling in plant defence response. CNGC19 is known to have cyclic nucleotide monophosphates (cNMPs) binding domain and calmodulin (CaM)-binding domain. CaMs are important calcium sensors that can bind to the carboxy tail of several plant CNGCs in Ca^{2+} dependent manner and regulate the opening and closing of channel. In Arabidopsis, out of all the CaM isoforms, CaM2 was highly upregulated by wounding and Spodoptera feeding and shows interaction with C-terminus of CNGC19. The objective of this project is also to overexpress and purify the CaM2 in order to study protein-protein interaction with its interacting partner CNGC19.

LIST OF FIGURES

List of Tables

CHAPTER 1

Introduction

Plants are the primary producers in food chain and most of the living organisms depend on them for their survival. Being sessile, plants are exposed to a large number of environmental stresses which adversely affect the agricultural productivity. These stress factors can be abiotic or biotic. Abiotic stress conditions include drought, salinity, temperature fluctuations, and many others leading to major crop loss worldwide. On the other hand, plants also encounter plethora of biotic stress factors including pathogens, fungus, insects and other heterotrophic organisms that depend on them for food and survival. In order to survive these stress conditions, plants have evolved complex defence mechanism at molecular and cellular levels (Erb and Reymond, 2019). Stress conditions triggers the activation of defence mechanism in plants which can be broadly categorised as constitutive defence and inducible defense (Wu and Baldwin, 2009). Constitutive defence constitutes the first line of defence by providing structural barrier to plants. Physical barriers including waxy cuticle, lignified cell walls, presence of thorns and trichomes reduces herbivore and pathogen attack (War et al., 2012). During inducible defence, plants sense the external stimuli (pathogens, microbes or insects) and generate an optimal response by producing toxic chemicals, secondary metabolites such as flavonoids, tannins, glucosinolates, reactive oxygen species or by emitting herbivore-induced plant volatiles that attract other enemies of the herbivores (Karban and Myers, 1989). Plant defence is activated upon sensing of elicitors called pathogen or microbe associated molecular pattern (PAMPs/MAMPs). These molecules are recognized by pattern recognition receptors (PRRs) and generate a general and non-specific basal immune response or PAMP-triggered immunity (PTI) (Nejat and Mantri, 2017). The response may also arise endogenously from host-plant derived signals known as DAMPs (damage associated molecular patterns) (Hou et al., 2019). In this co-evolutionary arms race of plants and microbes, pathogens release effector molecules which interfere with PTI and contributes to pathogen virulence giving rise to second level of immune response known as

effector triggered immunity (ETI) (Jones, J.D.G., 2006). This is specifically activated upon recognition of pathogen virulence factors released by the pathogens inside the cell (Cui et al., 2015). Recognition of these molecules by their cognate receptors activates many early signalling events like depolarisation of plasma membrane, increase in cytosolic concentration of calcium, ROS (reactive oxygen species) production and mitogen-activated protein kinase (MAPK) phosphorylation (Nejat and Mantri, 2017). Phytohormones like jasmonic acid (JA), ethylene (ET), salicyclic acid (SA) and abscisic acid (ABA) also plays crucial role in defence mechanism (Dodds and Rathjen, 2010).

1.1 Plant-insect interaction

The coexistence of plants and insects has been known for at least 350 million years and they have developed direct and indirect ways of interaction (Mithöfer and Boland, 2012). Insects are intimately associated with plants as they serve as a valuable source of shelter, food and site to lay eggs (Panda and Khush, 1995). This dynamic system of plant-insect interaction has also led to evolutionary arms race between them. Plants have evolved to develop various advanced strategies to overcome the challenges arising due to their continuous interaction with insects and defend themselves from herbivores (War et al., 2012). They have the ability to sense mechanical wounding and chemical cues elicited by herbivores and activate plant immune response. Plants defend themselves from herbivore attack directly through the presence of structural barrier or indirectly by attracting the natural enemies of herbivores (Aljbory and Chen, 2018). Plants recognizes herbivory on the basis of extent of physical tissue damage done by the insects. Herbivory is also perceived by herbivore cues present in saliva, oral secretions, ovipositional secretions of the insects and effectors (Wu and Baldwin, 2009).

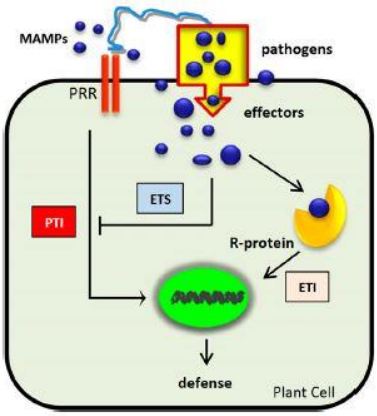

(a) (b)

Figure 1.1: Plant-pathogen interaction. (a) A plant pest *Spodoptera litura* (common cutworm) - feeding on leaf. (b) A general model for plant-pathogen interactions (Kazan and Lyons, 2014).

Plants sense herbivores and stimulate a large number of molecular events by activating receptor proteins, hormone signalling pathway, signal transduction cascades and transcription factors. In plants, wounding and herbivory by Spodoptera leads to the rapid activation of electrical signals. These events include electrophysiological response where upon insect attack, various electrical signal response is generated inside the plants such as action potential (AP), system potential (SP) and variation potential (VP) (Maffei et al., 2004). *Spodoptera littoralis* feeding leads to strong membrane depolarisation in *Phaseolus lunatus* (lima beans) leaves. *S. littoralis* feeding on plants also leads to herbivore-induced APs in *Vicia faba* and *H. Vulgare* (Zimmermann et al., 2016). Other reports shows that the larval feeding on plants, triggers SPs and alters the transmembrane potential (Vm) (Zimmermann et al., 2016).

In Arabidopsis, the electrical signals generated in response to wounded plant tissue activate long-distance signalling system. The wounded leaf perceives the tissue damage and results into the generation of signals by activating jasmonate biosynthesis which is then propagated to the other unwounded distal leaves connected by vasculature (Mousavi et al., 2013). Glutamate receptor- like (GLRs) genes are crucial for distal wound-stimulated expression of jasmonate signalling genes (JAZ) genes and propagation of the electrical signal to the distal leaves (Mousavi et al., 2013). Another important factor is calcium homeostasis. Calcium plays an important role in almost every aspect of plant development and signalling

pathways. In plants, response is generated against insect herbivory by inducing both local and systemic $[Ca^{2+}]_{cyt}$ signals which gets distributed within the vascular system. Spodoptera feeding on Arabidopsis showed elevation in systemic $[Ca^{2+}]_{cyt}$ calcium signals in the adjacent leaves directly connected to the treated leaf via vasculature (Kiep et al., 2015). TPC1, a Ca^{2+}-permeable vacuolar cation channel is promoted by the binding of Ca^{2+} to its cytosolic EF hands motifs (Peiter et al., 2005). The wound-induced signals generate systemic response which is regulated by TPC1-dependent Ca^{2+} release from vacuole which is supressed by insect-derived oral secretions (Kiep et al., 2015). Oral secretions from the larvae of generalist insect herbivore *S. littoralis* contains elicitors that induce transient calcium elevation in leaf disks and transient (+)-7-*iso*-jasmonoyl-L-isoleucine (JA-Ile) burst within minutes after application (Vadassery et al., 2012) (Kiep et al.,2015). Upon perceiving stress stimuli or herbivory, calcium is released from different calcium stores and leads to increase in cytosolic calcium level in the wounded leaf. Neomycin-phospholipase C inhibitor was identified to be involved in release of Ca^{2+} from internal stores such as vacuole and results into the elevation of Spodoptera-induced local $[Ca^{2+}]_{cyt}$ levels (Vadassery et al., 2019).

These external cues are sensed by the receptors/sensors present on the cell surface or cytoplasm and transferred to the transcriptional machinery situated in the nucleus. Production of secondary metabolites such as tannins, glucosinolates, flavonoids, phenols and many others act as toxic molecules and provide deterrence/anti-feedant activity or serves as precursors to various signalling events (Singha et al., 2011). Plants also produce various phytohormones like auxin, cytokinin, gibberellins (GA), abscisic acid (ABA), ethylene (ET), salicyclic acid (SA), jasmonates (JA) and other peptide hormones out of which SA, JA and ET are the three major phytohormones involved in regulating plant defence against pests and pathogens (Bari and Jones, 2009). Mechanical damage to plant tissue results in JA biosynthesis and its receptor-active derivative, jasmonyl-L-isoleucine (JA-Ile) and gives rise to JA-triggered immunity (JATI) (Kevin Range, 2012). This signal transduction leads to differential transcriptional change helping the plant to overcome the stress conditions by generating appropriate biochemical and physiological response.

1.2 Calcium signalling

Calcium serves as the universal and ubiquitous secondary chemical messenger involved in plants growth, development and signal transduction in plants (Hepler, 2005). Calcium also plays an important role in controlling membrane structure and function (Wyn Jones and Lunt, 1967; Burstrom, 1968). Cells are known to maintain a constant (low) level of cytosolic [Ca^{2+}] either by apoplastic export or by sequestering extra Ca^{2+} to the intracellular compartments with the help of Ca^{2+} transporters against the electrochemical gradient. Under various stress conditions, calcium level inside the cytoplasm increases either due to influx of calcium ions from extracellular environment or from intracellular compartments (Kiep et al., 2015). This rise in Ca^{2+} level concentration [Ca^{2+}] inside the cell is known as calcium signature (Marme and A.J. Trewavas, 1986).

In terms of Ca^{2+} influx, so far five protein families have been reported to transport calcium in plants, namely : Cyclic Nucleotide Gated Channels (CNGC), Glutamate like receptors (GLR) , Two Pore Channel (TPC), and reduced hyperosmolality-induced Ca^{2+} increase (OSCAs) (Edel et al., 2017). In *Arabidopsis,* GLRs, OSCAs, MID1-complementing activity (MCA) families and CNGCs are main plasma membrane calcium permeable channels, whereas TPC1 is the key vacuolar channel. Plants have many Ca^{2+} sensor proteins like calcineurin B-like (CBL) interacting protein kinases (CIPKs), Ca^{2+} dependent protein kinases (CDPKs) and calmodulins (CaMs/CaM-like (CMLs)) which then interacts with its interacting kinases and activates downstream defence signalling by regulating stress tolerance genes (Peiter, 2011); (Edel et al., 2017).

1.3 Cyclic Nucleotide Gated Ion Channels (CNGCs)

CNGCs belong to superfamily of multimeric voltage-gated cation channel family. They are localised in plasma membrane and has been identified in both plants and animals. It is involved in non-selective exchange of divalent and monovalent cations including Ca^{2+} and K^{+} across the membrane. CNGC have been identified as one of the important channel involved in conducting calcium during plant defence (Talke et al., 2003). CNGCs are tetrameric molecules and all the CNGCs has a pore forming domain containing glutamate residue which is responsible for calcium binding and blocking the flow of monovalent cations. The four repeated P-loops from 4 CNGC

monomers assembles into an inverted “tepee structure” and mediates the conduction of cations whereas the pore serves as selectivity filter (Ward et al., 2009). Each subunit of homotetrameric CNGCs contains intracellular N and C-termini, six transmembrane segments (TMs), a P region between TM5 and TM6 which acts as selectivity filter for the ions.

In animals, CNGCs were first identified in retinal photoreceptors and are involved in signal transduction of vertebrate visual and olfactory system (Zhang and Cote, 2005). Opening of the channel is regulated by the binding of cyclic guanosine/adenosine -3’, 5’ monophosphate (cGMP/cGMP) to the channel in dark allowing the influx of calcium ions. When light reaches retina, cGMP gets hydrolysed to GMP, due to which the cGMP level decreases in the cell, thereby shutting the channel. Closing of channel results into reduction of calcium level in the cell then acts as negative feedback in the signal transduction of visual system (Matulef and Zagotta, 2003). In animal CNGCs, calmodulin binding domain (CaMBD) is present in the amino (N) or carboxy (C)-terminus whereas cyclic nucleotide binding domain (CNBD) is present in the C-terminus. In animals, phototransduction in the retinal rods is controlled by cGMP-gated channel where calmodulin (calcium binding domain) inhibits the channel activity by binding to the β-subunit of the cytoplasmic N-terminus of the channel complex (Grunwald et al., 1998). CNBD is composed of two subunits: C-helix and roll sub domains which is further formed by two α-helices and 8 β-sheets between two helices. CNGCs in animals are more permeable to cations over anions. Apart from calcium, the channel also allows the exchange of monovalent cations (Kaupp and Seifert, 2002). Apart from this CNGCs has also been identified from olfactory bulbs, brain and other chemosensory tissues like spleen and muscles (Kaupp and Seifert, 2020); (Murphy and Isaacson, 2003).

On the other hand, plant CNGCs have been introduced very recently and has been suggested to form tetrameric channels (Chiasson et al., 2017). Electrophysiological analysis from *Xenopus laevis*, and complementation assays performed in various expression systems like *Saccharomyces cerevisiae* and *E. coli* indicates that some subunits of CNGCs have the ability to form functional homomeric (homotetramer or heterotetramer) channels (Kaplan et al, 2007; Chin et al, 2009). *Arabidopsis* genome consists of 20 CNGC family members that plays role against abiotic and biotic stress

(Maser, 2001). The sequence similarity of 20 CNGCs from *Arabidopsis thaliana* ranges from 55% to 83%. On the basis of sequence of amino acids, they are classified into four groups I, II, III and IV which is further subdivided into two sub-groups A and B (Meena et., 2019). Plant CNGCs are reported to be involved in various growth and physiological processes of plants. The first CNGC identified from plants was *Hordeum vulgare* calmodulin binding transporter 1 (HvCBT1) from barley (Schuurink et al., 1998). They have been identified to play a key role in hormone responses, symbiosis, circadian rhythm (Jammes et al., 2011). There are reports showing that plant CNGCs are involved in gibberellic acid-induced signalling in aleurone development (Penson et al., 2016). Unlike animals, plants have been reported to have CaMBD located in the C-terminus. CaMBD of AtCNGC1 localized in the α-helix of putative CNBD suggests that this overlapping of CaMBD with CNBD is conserved between plants and animals. AtCNGC1 and AtCNGC2 shows difference in calmodulin binding affinity among multiple isoforms of calmodulin (Köhler and Neuhaus, 2000).

1.4 Functional role of plant CNGCs

CNGCs are known to be involved with various roles ranging from growth and development, nutrient uptake, ion homeostasis, plant immunity to stress tolerance. AtCNGC10, a putative K^+ channel localised in plasma membrane modulates cellular K^+ level across the membrane and is involved in growth and development of plants (Borsics et al., 2007). AtCNGC16 gene is believed to be critical for pollen fertility under heat stress and drought conditions (Tunc-Ozdemir et al., 2013a). In rice, it was observed that among 16 OsCNGCs, the expression level of 10 OsCNGCs (OsCNGC6 having highest expression of 192-folds) was highly upregulated under cold stress (Nawaz et al., 2014). *CNGCb* gene from *Physcomitrella patens* and its Arabidopsis ortholog CNGC2 responds to increase in ambient temperature conditions and imparts thermotolerance in plants (Finka et al., 2012). Arabidopsis CNGC1 confer Pb^{2+} tolerance by acting as active component in the transport pathway and mediating the entry of Pb^{2+} into the plant cell (Sunkar et al., 2000). AtCNGC4,a close paralog of AtCNGC2 work synergistically and are involved in plant defence and flower transition (Chin et al., 2013). CNGC7 and CNGC8 share 74% protein sequence identity and plays a crucial role in the initiation of growth of pollen

tube tip (Tunc-Ozdemir et al., 2013b). AtCNGC17 coexpresses with phytosulfokine (PSK) and regulates the growth of seedlings (Ladwig et al., 2015). Four CNGC channels (CNGC 2, 4, 11, 12) have been well studied for their role in DAMP-triggered and R-gene-mediated immune responses (Clough et al., 2000) ; (Balagué et al., 2003). In Arabidopsis, there are various instances showing that loss-of -function studies in CNGCs has revealed altered plant responses against pathogens. Mutants identified from AtCNGC2 (*dnd1*-''defense, no death'') and AtCNGC4 *dnd2* exhibits loss of hypersensitive response (HR) cell death and serves as efficient tool for the dissection of mechanism behind plant defense signalling (Clough et al., 2000)(Jurkowski et al., 2004). AtCNGC11/12 – a novel chimeric gene generated by fusing two AtCNGC encoding genes with *cpr22* (mutant constitutive expresser of PR genes22) forms a functional cAMP-activated CNGC and identified as positive mediators providing resistance against *Hyaloperonospora parasitica* (Yoshioka et al., 2006).

1.5 Cyclic Nucleotide Gated Channel 19 (CNGC19) in plant - biotic interactions

CNGC19 is wound and herbivore activated gene belonging to group IVa of CNGC family. It has been identified as an important plasma membrane localized channel and having key functional role in calcium mediated defence mechanism against *Spodoptera litura* in Arabidopsis (Meena et al, 2019). Whole genome transcriptome analysis showed elevated expression of Cyclic Nucleotide Gated Channel 19 (AtCNGC19) upon wounding and oral secretion treatment locally as well as systemically. Upon stimulation with oral secretion of *S. litura*, CNGC19 transcript level was elevated in as early as 15 minutes and peaked at 1-hour. CNGC19 is rapidly activated and needed for optimal vasculature-based spread of Ca^{2+} upon wounding. Loss of CNGC19 function results in decreased herbivory defense and increased Spodoptera feeding. Jasmonic acid dependent signalling cascade is highly crucial for plant defense against herbivores. CNGC19 was found to be jasmonate regulated and *CNGC19* loss-of-function affected jasmonate signalling upon herbivory. Loss of *CNGC19* results in decreased herbivory defence and aberrant wound-induced Ca^{2+} signalling. Loss-of-function of *CNGC19* shows a reduced aliphatic glucosinolate (plant defense compound) and increased methionine levels via an effect on chain elongation pathway of Met-derived glucosinolate. It is also

involved in the perception of DAMP (Pep) and regulated by PEPR during the early stages of herbivory (Meena et al., 2019). The role of CNGC19 has also been discovered in legume-rhizobia symbiosis and nodulation. Rhizobia bacteria are recognized by plant via Ca^{2+} oscillations in the nucleus and perinuclear region. A brush mutant isolated from *Lotus japonicas* exhibits defect in nodule development due to leaky Ca^{2+} channel, and is an orthologue of CNGC19 from Arabidopsis (Chiasson et al., 2017). CNGCs in *Medicago truncatula* are also involved in generation of nuclear Ca^{2+} spike, which is crucial in interaction with symbiotic mycorrhizal fungi (Charpentier et al., 2016). A recent study shows that CNGC19 upon colonisation with *Piriformospora indica*,a root endosymbiont provides robust innate immunity and is important for growth-promotion signalling (Jogawat et al., 2020). In spite of available knowledge, the synthesis and mechanism of CNGC19 mediated defense remains unexplored. Further studies on CNGC19 to reveal its structure might help in better understanding of its biochemical and biophysical properties.

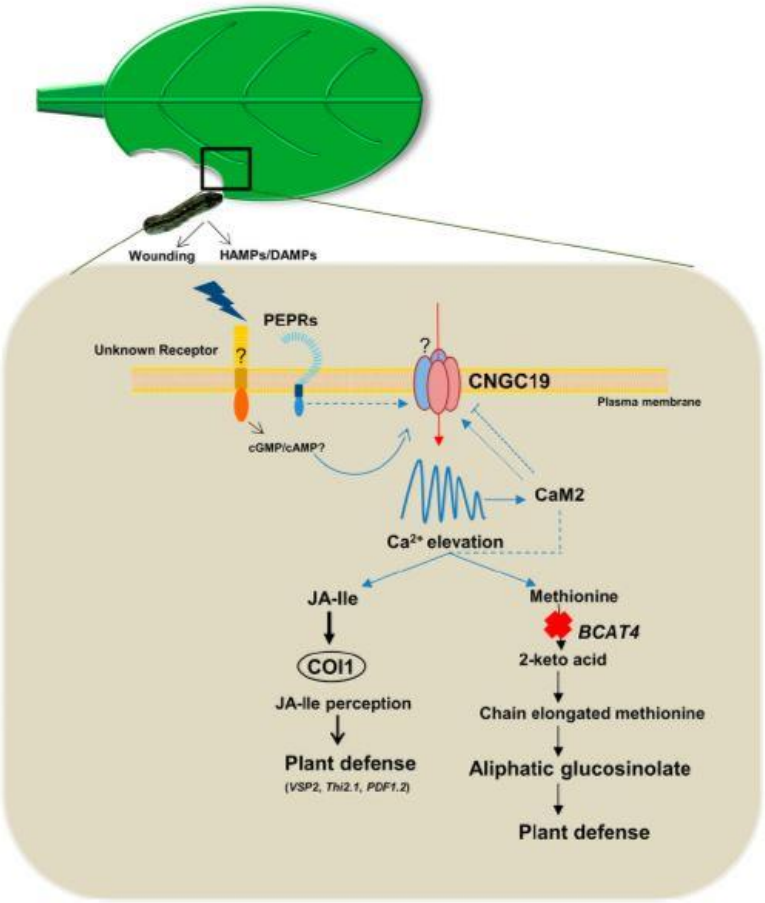

Figure 1.2: Model for a Role of Arabidopsis CNGC19 in Plant Defense against *S. litura* Herbivory (Meena et al., 2019).

1.6. Structure and function of CNGC19

Cyclic nucleotide gated channels are voltage-independent and has six transmembrane (TM) having a pore forming domain between TM5 and TM6.

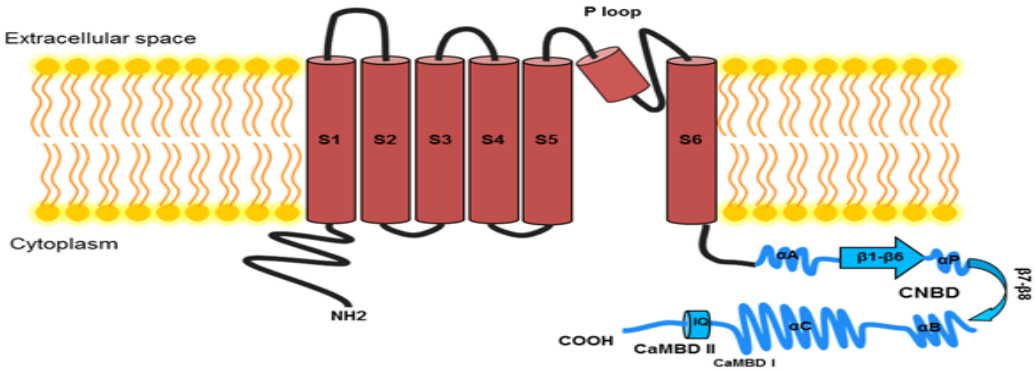

Figure1.3. The topological model of plant CNGC19 (Meena and Vadassery, 2018).

CNGC19 are heterotetrameric proteins having cytosolic N-terminal domain followed by six membrane-spanning segments from S1-S6. A pore forming domain is present between S5 and S6 known as P-loop which acts as a selectivity filter for the ions passing through. The transmembrane domains are followed by C-terminal having two important binding domains cyclic nucleotide binding domain (CNBD) and calmodulin binding domain (CaMBD)(Mühlberger, 2013); (Véry and Sentenac., 2002). In animal CNGCs, CaMBD is present at N-terminal whereas in plants, CaMBD is at C-terminal (Zagotta and Siegelbaum, 1996; Bradley et al., 2004; Trudeau and Zagotta, 2003). C-linker acts as linker between C-terminal and transmembrane domain. CaM domain also has Isoleucine-Glutamine (IQ) domain which is involved in binding with calmodulin (Fischer et al., 2013). Binding of monophosphates (cGMP and cAMP) leads to the allosteric change in the holoenzyme thereby rotating the P-loop and facilitating permeation through the channel (Flynn *et al*., 2001). The channel is activated by binding of cyclic nucleotide monophosphates (cAMP/cGMP) to the cyclic nucleotide binding domain (CNBD) which results into opening the channel. Upon stress conditions, due to increase in calcium level, calcium ions bind to calmodulins (CaM) which further binds to CaM

binding domain (CaMBD). According to the traditional model, binding of Ca^{2+}/CaM2 to CaMBD prevents cNMPs from binding the channel, thereby closing the channel (Meena et al., 2019). Upon insect attack, the channel also interacts with CaM2 to induce the downstream defense signalling (Meena et al., 2019).

Hence by determining the structure of CNGC19, we can understand the exact mechanism by which CNGCs couples channel activation to downstream defence.

1.7 Role of Calmodulins (CaMs) in regulating CNGCs

CaMs are one of the reported calcium sensors which is evolutionary conserved protein. CaMs have EF- hand motifs that can bind to calcium ions. Upon increase in calcium levels, CaM binds to Ca^{2+} and undergoes conformational change leading to interaction with the target proteins (Fernandes and Oliveira-brett, 2017). There are many calmodulin isoforms reported from plants. In *Arabidopsis*, there are four different highly conserved isoforms of CaM – CaM1/CaM4, CaM2/CaM3/CaM5, CaM6 and CaM7 encoded by seven CaM genes (Mccormack et al., 2003). CaM and CMLs are well-known calcium sensors involved in regulating the growth, development and stress responses of plants. CaMs have been shown to bind to carboxy tail of several plant CNGCs in a Ca^{2+}-dependent manner and further regulate the opening and closing of the channel (Fischer et al., 2017). Upon stimulated herbivory, it was found that CaM2 was highly upregulated by wounding and OS secretion of *S.litura*. In response to this, the interaction of CNGC19 C-terminus was tested with the four isoforms of Arabidopsis CaM by yeast two hybrid (Y2H). It revealed that CNGC19 shows interaction with CaM2, CaM3, CaM6 and CaM7 (Fischer et al., 2017). This was also confirmed with BiFC experiment (Meena et al., 2019). There are also reports that CaM can positively and negatively regulate CNGC12. Similar to CNGCs in animals, Arabidopsis CNGC12 possess multiple CaMBDs at both cytosolic N and C termini where apoCaM interaction with conserved IQ motif present in the C-terminus regulates the channel function whereas Ca^{2+}/CaM binds additionally to the N- and C-terminal motifs with different affinities (DeFalco et al., 2016).

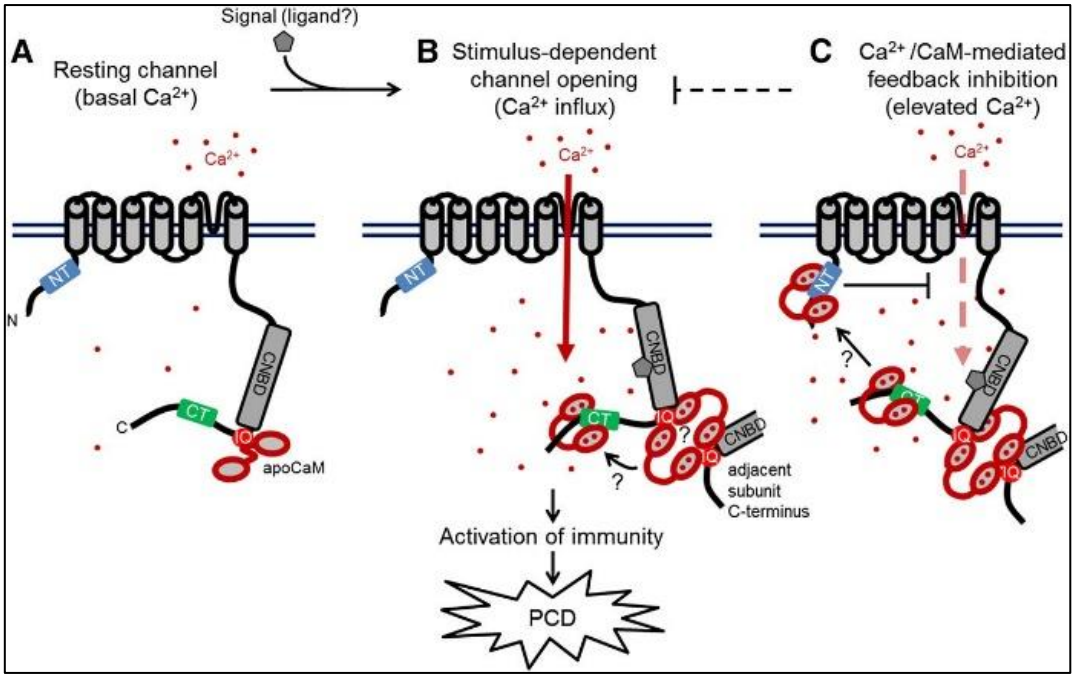

Figure 1.4: Proposed model of CNGC12 regulation by CaM (DeFalco et al., 2016)

CNGC18, CNGC8 and CNGC7 together with CaM2 constitute a molecular switch that regulates the opening and closing of calcium channel depending on the level of calcium. The channel opens when under low calcium level, calcium free CaM2 (Apo-CaM2) interacts with CNGC18-CNGC8 complex whereas upon increase in the calcium level, calcium bound CaM2 dissociate from the complex thereby closing the channel (Pan et al., 2019).

1.8 Expression and purification of membrane proteins

The expression and purification of the membrane proteins is considered as one of the most powerful technique required to solve its structure. We aim to solve the structure of CNGC19 and hence membrane protein purification and expression is crucial. Proteins of interest are expressed, purified and characterized using conventional and molecular biological approaches and methods. They have wide applications not only in research and biotechnology but also in medicine. The progress of purification of membrane protein is slow and challenging as it requires development of methods and strategies to express and isolate proteins. The biochemical characterisation of the membrane proteins becomes difficult because of their certain unique properties: low abundance of membrane proteins in biological membranes, embedded in lipid bilayers and often not generally soluble in aqueous

solutions, tend to form aggregates and might associate with other proteins to form larger complex (Gürbilek, 2013).To overcome this, several experimental methods have been devised to purify membrane proteins. Membrane associated domains are amphipathic and can be solubilized using appropriate detergents. Detergents helps in releasing the membrane associated regions by forming micelles (Orwick-Rydmark et al., 2016). However, detergent effects the physiochemical properties of the desired protein and screening of various detergents are carried out to successfully optimize the solubilization of membrane proteins. To maintain the solubility of membrane protein in aqueous buffer, nonconventional surfactants are also being used (Systems et al., 2004). There are reports showing that addition of polyamines, alkylamines such as ethylammonium nitrate along with the detergent helps in intensifying the solubilization of membrane proteins. These molecules prevent hydrophobic membrane proteins from getting aggregated and their interaction with phospholipids (Yasui et al., 2010).

Expression of the protein requires an appropriate expression system. There are different expression systems available – 1) Bacterial system - most common of which is *E. coli-based* expression system. Bacterial system is more preferably used expression systems to express and purify recombinant proteins because of its properties like – easy to culture, rapid growth and production yield is more. However, eukaryotic protein expression in prokaryotes like bacteria is most often non-productive as they fail to have machinery required for post translational modifications. 2) Yeast system is the most widely used system for the expression of eukaryotic proteins. Being unicellular and eukaryotic organism, yeast is easy to culture, has resistance to chemical and secondary metabolites. Apart from this, it also has membrane-bound compartments and complete sub-cellular organelles which helps in efficient folding of eukaryotic proteins (Huang et al., 2014). This system has been used for structure determination of TPC1 channel in Arabidopsis (Chimbindi et al., 2016). 3) Mammalian cells -are used for post translationally modified proteins like glycosylated proteins, phosphorylated proteins or the proteins which are insoluble. Protein production in mammalian cells offers the advantage of providing environment similar to wild type for efficient transcription, translation accompanied with relevant chaperones, post translational modifications leading to the production of functionally active proteins (Hunter et al., 2019). While purifying the

proteins certain parameters should be considered such as – isoelectric point (pI). These approximate values are useful for selecting the pH of the buffers and ion-exchange resins. Post-translational modifications such as phosphorylation and glycosylation might affect the pI and thereby hamper the protein production (Widmann et al., 2010). Another major factor having a crucial role in heterologous gene expression in any other host system is codon optimization (Burgess-Brown et al., 2008). Expression of eukaryotic protein in bacterial expression host such as *E.coli* severely limits the translation process due to non-availability of less frequent tRNAs. This often results into frame shift mutations, termination and thus leading to low protein production (Chen, 2012). To overcome this limitation, the target gene is codon optimized or tRNA enhanced strains are used for the possible expression of heterologous proteins in *E.coli* (Burgess-Brown et al., 2008). The protein of interest is tagged with epitope tags to either N- or C- terminus (or both) which facilitates the purification of fusion proteins (Tuteja and Mahajan, 2007; Uhlen et al., 1992; Makrides, 1996). These tags are linked to the desired protein of interest via short linker sequence having a cleavage site. The most commonly used tags are poly-histidine tag (His-tag) and the glutathione-S-transferase (GST-tag). A tag may help maintain the solubility of a protein that is normally expressed in an insoluble form (La Vallie et al., 1993; Zhang et al., 1998).

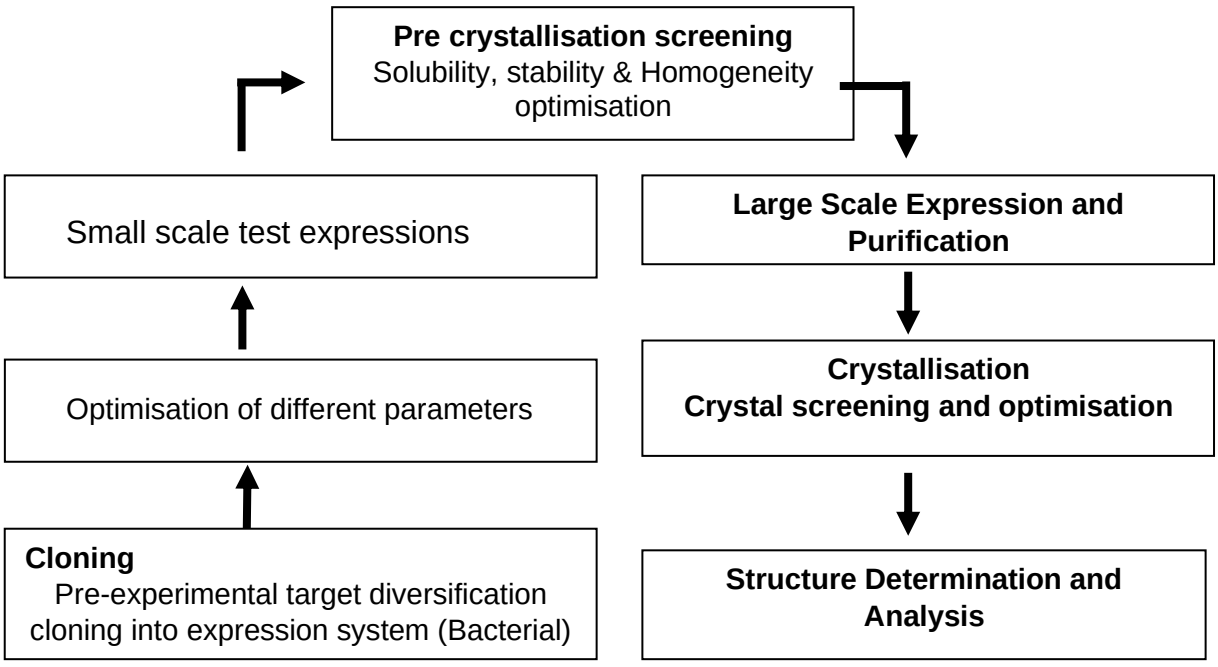

Figure 1.5: Flowchart representing the steps followed in expression and purification of membrane protein.

1.9. Bacterial protein expression

Bacterial system is more preferably used expression systems to express and purify recombinant proteins because of its properties like –fast growth kinetics, high yield (Rosano and Ceccarelli, 2014). However, eukaryotic protein expression in prokaryotes like bacterial system is most often non-productive as they fail to have machinery required for post translational modifications. *E.coli* is the most commonly used expression system for the production of heterologous proteins. Bacteria being simple organisms have extremely efficient gene regulation machinery. They can withstand variety of environments by responding with complex regulatory mechanisms. Bacteria synthesize proteins depending on the carbon sources and other nutrients available in the environment by altering their gene expression pattern. Bacterial genes are clustered into clusters of co-regulated genes (operons) which are under a common control mechanism. One such operon present in *E.coli* bacteria is lactose (lac) operon (Browning et al., 2019).

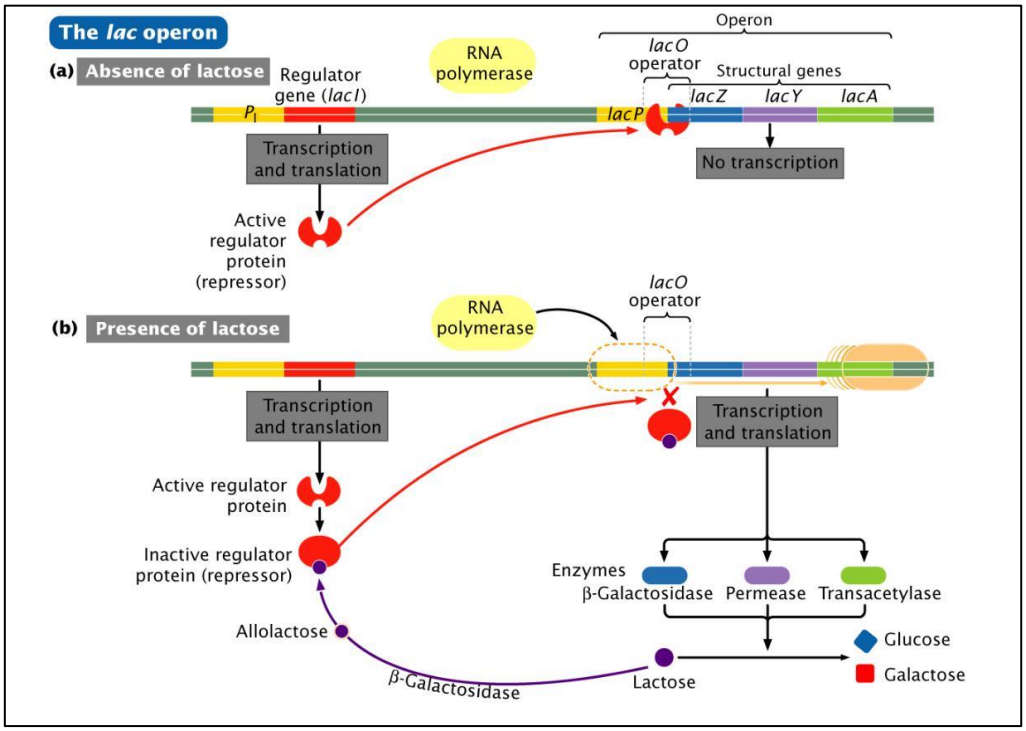

Figure 1.6 Gene Expression Machinery – Lac operon

Lac operon is comprised of three structural genes *lacZ* encoding beta-galactosidase, *lacY* encoding permease and *lacA* encoding transacetylase. These genes together encode for proteins involved in lactose metabolism and helps in breakdown of lactose for easy uptake by the cells (Stoebel et al., 2008). These structural genes lie on the same continuous stretch of DNA and are downstream of a single promoter which serves as a recognition site for the transcriptional machinery of the RNA polymerase complex. In addition to the structural genes, lac operon also includes operator present between promoter sequence and structural genes, and terminator which ensures coordinated control of bacterial gene expression machinery (Browning et al., 2019). Plant CNGCs have never been crystallized. I attempt to express and purify the cytosolic N and C terminal of CNGC19.

Aims and Objectives

1. **Overexpression of cytosolic domains of CNGC19 in suitable expression system.**

   To overexpress the cytosolic domains (N and C-terminal) of CNGC19 using appropriate vector and expression host system.

2. **Optimization of conditions for protein overexpression.**

   To optimize parameters like *E. coli* strain, temperature, IPTG concentration, incubation time period and buffers for the optimal expression of protein.

3. **Purification of the cytosolic domains for structural studies.**

   Large scale expression of N-terminal and C-terminal domains of CNGC19 by using optimized conditions and purifying proteins using affinity and size exclusion chromatography to carry out structural studies and protein-protein interaction.

4. **Expression and purification of CaM2.**

   To purify CaM2 in order to study protein-protein interaction with its interacting partner CNGC19

CHAPTER 2

Materials and methods

2.1 Cloning of the cytosolic domains of CNGC19 into suitable vector and expression system.

The nucleotide sequence of Arabidopsis CNGC19 full length having 728 amino acids was retrieved from TAIR (www.arabidopsis.org). Three different constructs were prepared for the over-expression of cytosolic domains of CNGC19 in *E. coli*- N-terminal domain having 156 amino acids (17.3 kDa), C-terminal-I without C-linker having 201 amino acids (23 kDa) and C-terminal-II with C-linker having 245 amino acids (29kDa).

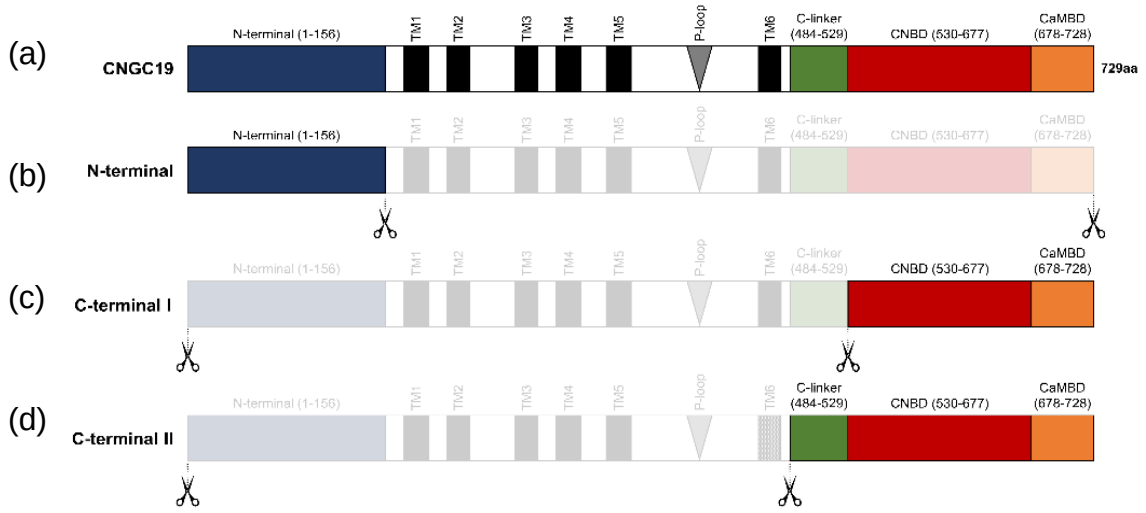

Figure 2.1: Domain architecture of the constructs designed to overexpress the cytosolic domains (a) CNGC19 full length having 729 aa (b) N-terminal (from 1-156 aa) (c) C-terminal I (from 530-728aa) (d) C-terminal II (from 484-728aa)

S.no	Cytosolic domain	Amino acids	Mol.wt. (Da)	pI	Extinction coefficient ($M^{-1}cm^{-1}$)
1	N-terminal	408	46421.83	8.47	63300
2	C-terminal I	452	52451.36	8.31	72685
3	C-terminal II	499	58378.22	8.99	85175
4	CaM2	412	47079.56	4.89	51590

Table 2.1: Summary of the derived physio-chemical properties of the cytosolic domains of CNGC19 expressed in *E.coli.*

Restriction digestion-based cloning was done using *NcoI*/*XhoI* restriction enzymes. In order to express these cytosolic domains, the constructs were cloned into pETM30 expression vector having 6346 bp containing 6x His-tag followed by the TEV protease cleavage site and GST tag. Clones were confirmed by restriction digestion and DNA sequencing (Macrogen). The construct used for this experiment were already cloned and available in the lab.

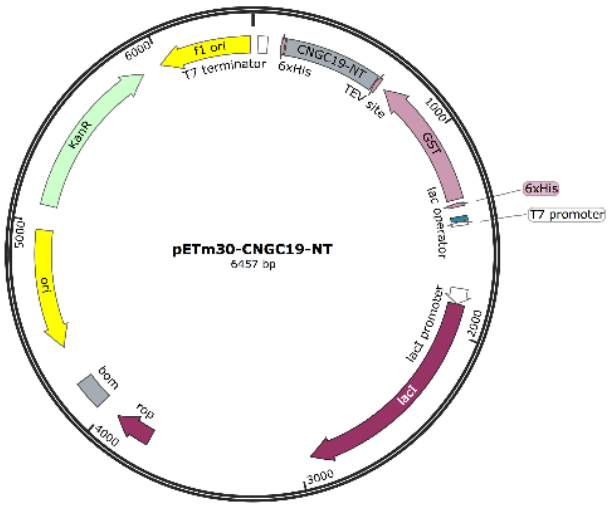

(a)

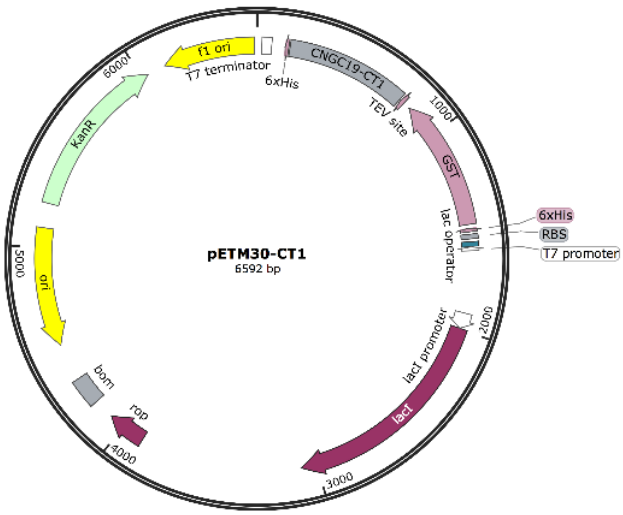

(b)

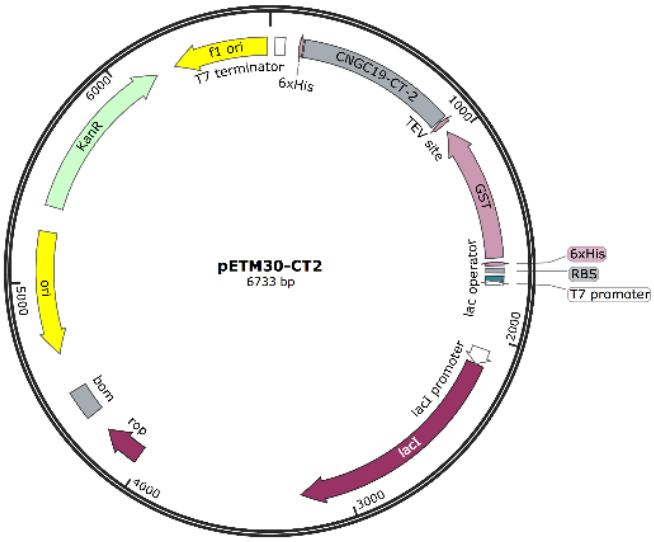

(c)

Figure 2.2: Vector map showing cytosolic domains cloned in expression vector pETM-30 (a) N-terminal domain having 6xHis-tag followed by TEV cleavage site and GST tag (b) C-terminal I (c) C-terminal II

2.2 Preparation of competent cells

Rosetta™2 (DE3) pLysS cells were streaked on Luria-Bertani (LB) agar plate supplemented with chloramphenicol (34mg/ml) antibiotic and incubated at 37ºC overnight. Primary culture was inoculated by adding a single colony from the streaked plate to 100 ml of LB media and incubated at 37ºC, 130 rpm shaker until OD_{600} reaches 0.4-0.6. As soon as $O.D_{600}$ reached 0.6, the culture was incubated in ice for 15 minutes. Centrifuge the cells at 4,000 rpm, 4ºC for 10-15 minutes and

discard the supernatant. Resuspend the pellet obtained in 20 ml of transformation buffer (Tfb-I) containing 1M CH_3COOK, 1M $MnCl_2$,1M $CaCl_2$ and 50% glycerol, pH adjusted to 5.8. Spin the cells at 4,000 rpm for 10 minutes at 4ºC and discard the supernatant. Resuspend the pellet in 4 ml of Tfb-II containing 1 M MOPS, 1M $CaCl_2$, 1M KCl and 50% glycerol and immediately aliquot 50µl each into pre-chilled 1.5 ml microcentrifuge tubes (MCTs), flash freeze in liquid nitrogen and store them at -80ºC. Highly efficient competent cells were also prepared for BL21 (DE3) using similar procedure.

2.3 Transformation of E. coli

For transformation, ~100ng (1 µl) of plasmid was added to the three different *E.coli* strains (Rosetta™2 (DE3) pLysS and BL21 (DE3)) followed by gently mixing and incubation in ice for 30 minutes. Transformation was performed using heat shock method by keeping the cells into water bath pre-set at 42ºC for 90 seconds and then immediately transferring into ice for 5 minutes. 950 µl of LB was added to the cells and further incubated at 37ºC incubator with constant shaking at 130 rpm for 1 hour. Cells were centrifuged at 5,000 rpm for 5 minutes and 900 µl of the supernatant was discarded. The remaining 100 µl of the cells were then further plated on LB agar plates supplemented with appropriate antibiotics (Rosetta™2 (DE3) pLysS - kanamycin and chloramphenicol and BL21 (DE3)-kanamycin) and incubated at 37ºC overnight.

2.4 Media preparation

For the small-scale test expression of cytosolic domains, four different types of media were used i.e. LB-broth, LB-Lennox, autoinduction media and 2XYT having following composition as mentioned in Table 2.2. Media was prepared using Milli-Q and autoclaved at 121ºC for 30 minutes.

Components/ 100ml	**LB**	**Lennox**	**Autoinduction**	**2XYT**
Tryptone	1g	1g	1g	1.6g
NaCl	1g	0.5g	-	1g

Yeast Extract	5g	0.5g	0.5g	0.5g
(NH4)2SO4	-	-	0.33g	-
KH2PO4	-	-	0.68g	-
NA2HPO4	-	-	0.71 g	-
Glucose	-	-	0.05g	-
MgS04	-	-	0.015g	-
8% w/v lactose	-	-	0.2 g	-

Table 2.2: List of components used in the preparation of different kinds of media.

LB agar was prepared by adding 2.5g of LB and 1.5g of agar per 100 ml and autoclaving at 121ºC for 30 minutes. LB agar plates were prepared by adding appropriate antibiotics (Rosetta™2 (DE3) pLysS- kanamycin + chloramphenicol and BL21(DE3)- kanamycin).

2.5 Optimisation of different parameters for protein overexpression

Small scale expression was done by varying different parameters such as media, bacterial strain, temperature, IPTG concentration and buffer to optimize an appropriate condition of the protein expression.

2.5.1 Optimisation of conditions for CNGC19 N-terminal domain (1-156aa)

S. no	Strain	Temp. (ºC)	IPTG conc. (mM)	Incubation time (hours)	Media	Buffer
1	Rosetta2 (DE3) plysS and BL21 (DE3)	20, 25 and 37	0.4 and 1	16, 12 and 4	LB	Lysis Buffer
2	Rosetta2 (DE3) plysS and BL21(DE3)	20 and 25	0.4	16, 12	LB	Lysis buffer (+/-glycerol)
3	Rosetta2	20 and 25	0.1 and	16, 12	LB	Lysis buffer+

	(DE3) pLysS		0.4			Triton-X-100(+/- glycerol)
4	Rosetta2 (DE3) pLysS	16 and 20	0.4 mM	18 and 16	LB, Lenox, 2XYT, Autoinduction	Lysis buffer

Table 2.3: Summary of different conditions used for the small-scale test expression of N-terminal domain.

2.5.2 Optimisation of conditions for CNGC19 C-terminal domain (530aa – 728 aa)

S.no	Strains	Temp.	IPTG conc.	Incubation time	Buffer
1	Rosetta2 (DE3) plysS and BL21 (DE3)	20, 25 and 37	0.4 mM and 1 mM	16, 12 and 4 hours	Lysis Buffer
2	Rosetta2 (DE3) plysS and BL21 (DE3)	16 and 20	0.4 mM	18 and 16 hours	Lysis Buffer
3	Rosetta 2 (DE3) plysS	20	0.25 mM	5 ,10 and 16 hours	Lysis Buffer
4	Rosetta2 (DE3) pLysS	16	0.05 mM	3 days	Lysis Buffer + Sodium cholate + DTT

Table 2.4: Summary of different conditions tested for the small-scale test expression of C-terminal domain.

2.5.3 Optimisation of conditions for CaM2

S.no	Strain	Temp.	IPTG conc.	Incubation time	Buffer

1	Rosetta2 (DE3) pLysS	16	0.05mM	3 days	Lysis Buffer + Sodium cholate + DTT

Table 2.5: Summary of different conditions tested for the small-scale test expression of CaM2.

2.6 Small-scale test expression of the cytosolic domains (N-terminal, C-terminal) and CaM2

Small scale pilot test expression was carried out, to test multiple parameters for the optimisations of conditions suitable for protein expression of both cytosolic domains and CaM2. Transformation was done in different *E.coli* strains [Rosetta2 (DE3) pLysS, BL21 (DE3) and Shuffle T7 Express *lysY*] using heat shock method. The transformed colonies obtained were inoculated into 10 ml of LB media supplemented with appropriate antibiotics as primary culture and further incubated at 37ºC, 130 rpm shaker till OD_{600} reached 0.4-0.6. Secondary culture was inoculated by adding 1% of this primary inoculum to 25 ml of LB media supplemented with antibiotics and incubated at 37ºC till OD_{600} reached 0.4-0.6. When OD reaches 0.6, the temperature of the flasks was allowed to cool down by keeping them at 4ºC for 10-15 minutes. IPTG was added and kept in pre-set incubator with constant shaking for the conditioned incubation time period.

2.7 Small-scale purification of the cytosolic domains and CaM2 using Ni^{2+} -NTA (nitrilotriacetic acid) affinity chromatography

After the growth of cells for the required time period, cells were harvested by centrifuging at 3500rpm, 4ºC for 20 minutes and supernatant was discarded. The pellet obtained was resuspended in lysis buffer in the ratio of 1:10 and cells were lysed using freeze thaw method by freezing the lysate in liquid nitrogen and then immediately transferring to water bath set at 37ºC. This cycle was carried out thrice for proper lysis. The lysate was then further centrifuged at 13,000 rpm, 4ºC for 40 minutes.

Batch binding was done using QaigenNi^{2+} Resin. Ni resin was equilibrated with 5 column volumes (CV) of equilibration buffer (Tris pH-7, 10% glycerol, 300mM NaCl, 10mM Imidazole). A slurry of 100 µl containing Ni-NTA matrix was added to the obtained supernatant for overnight binding at 4ºC. Next day, the unbound protein (flow through) was collected by spinning the supernatant containing Ni sepharose beads at 500 rpm for 5 minutes at 4ºC. The beads were then washed with 1 ml of wash buffer (Tris pH-7, 10% glycerol, 300mM NaCl, 10mM Imidazole) twice to remove non-specifically bound proteins. The protein was further eluted in 100 µl of elution buffer (Tris pH-7, 10% glycerol, 300mM NaCl, 500mM Imidazole). The samples were collected and run in duplicates to check on 15% SDS -PAGE for coomassie as well as for western blot analysis.

2.8 Large scale overexpression of C-terminal I and CaM2

2.8 a) Transformation

Transformation was done by using 1 µl of C-terminal I plasmid without C-linker having aa into Rosetta2 (DE3) pLysS competent cell followed by gently tapping as mentioned in (2.2.2). Heat shock treatment was given by keeping the cells into water bath pre-set at 42ºC for 90 seconds and then immediately transferred to ice for 5 minutes. 950 µl of LB was added to the cells and further placed in 37ºC shaker 180 rpm for 1 hour. Cells were centrifuged at 5000 rpm for 5 minutes. 100 µl of it was then further plated on LB agar plates supplemented with kanamycin (50 mg/ml) for the vector and chloramphenicol (34 mg/ml) and kept at 37ºC overnight.

2.8 b) Media preparation and IPTG induction

100 ml of LB media for primary culture was prepared in MilliQ and autoclaved at 121ºC for 30 minutes. For CaM2, 4 litres of LB media was prepared and divided into twelve 1 L baffled flasks each containing 660 ml of culture. While C-terminal was overexpressed using 8 litres of bacterial culture.

Primary culture was inoculated by adding scrap from the plate containing transformed colonies into flask containing 100ml of LB media supplemented with kanamycin and chloramphenicol and then incubated at 37ºC, 130 rpm shaker till OD_{600} reaches 0.4-0.6. Secondary culture was inoculated by adding 1% of this

primary culture into each flask containing 660 ml of LB media supplemented with kanamycin and chloramphenicol and incubates the flasks at 37ºC; 80 rpm shaker till OD_{600} reaches 0.4-0.6. As soon as OD reaches, the temperature of the culture was allowed to cool down by keeping them at 4ºC (cold room) for 10-15 minutes.
Secondary culture was induced with 0.05 mM of IPTG concentration and kept in pre-set incubator at temperature 16ºC with constant shaking at 80 rpm for 3 days.

2.8 c) Cell Lysis

After 3 days, cells were harvested by centrifuging the culture in sorvall bottle at 3500 rpm at 4ºC for 20 minutes. Weight of the pellet was recorded and stored at -20ºC after flash freezing in liquid nitrogen. The pellet obtained was thawed on ice and fresh lysis buffer was prepared. Pellet was dissolved in the ratio of 1:10 of ice-chilled lysis buffer containing 50 mM Tris pH-7, 300 mM NaCl, 10% Glycerol, 1% Triton-X-100, 1 mM Benzamidine HCl, 1 mM PMSF, 2 mM MgCl2, 10 µg/ml DNase-I,100 µg/ml Lysozyme, 1 mM DTT and 100 mg/l sodium cholate. (Cell lysis for C-terminal I was carried out using lysis buffer in the ratio of 1: 5). Cell lysis was performed by using bead beater pre-equilibrated with equilibration buffer (50 mM Tris, 300 mM NaCl, 10 mM imidazole and 10% glycerol) following 1 minute on and then five minutes off cycle for 5 times. The lysate was then transferred to clean Oakridge tubes and centrifuged at 13,000 rpm for 40 minutes at 4ºC. Pellet and supernatant were obtained and 100 µl of sample was collected for examining in SDS-PAGE and western blot.

2.8 d) Large scale purification of C-terminal I (530-728aa)

Immobilized metal affinity chromatography (IMAC) was carried out using GE Ni^{2+}Sepharose™ HisTrap™ excel 5 mL column pre-equilibrated with equilibration buffer (Tris pH-7, 10% glycerol, 300 mM NaCl and 10 mM Imidazole). To the supernatant, 10 mM of imidazole was added and using peristaltic pump it was passed through the recharged columns at very slow flow rate of 0.5 ml/min in loop to ensure efficient binding of the protein and flow through was collected containing the unbound protein. Subsequently, the columns were disconnected from peristaltic pump and connected to FPLC AKTA and the columns were washed with 5 CVs of wash buffer I (50 mM Tris, 300 mM NaCl, 10% glycerol and 10 mM imidazole) and 5

CVsof wash buffer II (50 mM Tris, 300 mM NaCl, 10% glycerol and 20 mM imidazole) to remove the non-specifically bound proteins.

Gradient elution was performed using elution buffer containing Tris pH-7, 10% glycerol, 300 mM NaCl, and 10 mM/ 500 mM Imidazole. The fractions were eluted with fraction size of 3ml and protein concentration was estimated using Bradford's method.

2.8 e) Large scale purification of CaM2

Immobilized metal affinity chromatography (IMAC) was carried out using GENi^{2+} Sepharose™ HisTrap™ excel 5 mL column pre-equilibrated with equilibration buffer (Tris pH-7, 10% glycerol, 300 mM NaCl and 10 mM Imidazole). To the lysate supernatant, 10 mM of imidazole was added and using a peristaltic pump it was passed through the recharged columns at very slow flow rate of 0.3 ml/min in loop to ensure efficient binding of the protein and flow through was collected containing the unbound protein. Subsequently the columns were disconnected from peristaltic pump and connected to FPLC- AKTA, the columns were washed with 5CVs of wash buffer I (50 mM Tris, 300 mM NaCl, 10% glycerol and 10 mM imidazole) and 5 CVs of wash buffer II (50 mM Tris, 300 mM NaCl, 10 % glycerol and 20 mM imidazole) to remove the non-specifically bound proteins.

Gradient elution was performed using elution buffer containing Tris pH-7, 10% glycerol, 300 mM NaCl, 10 mM/500 mM Imidazole. The fractions volume collected was 1 ml, and protein concentration was estimated using Bradford's method.

2.8 f) TEV cleavage and dialysis

Protein containing fractions obtained after gradient elution were pooled and 5 mM DTT and 2 mM EDTA was added. Dialysis was performed pipetting the by the pooled protein in a 3,500 MWCO dialysis bag (Thermo Scientific) and adding TEV enzyme in the ratio of (1:15) to cut 6x His tag. The bag was placed in dialysis buffer I (300 mM NaCl, 5 mM DTT, 2 mM EDTA and 50 mM Tris (pH7)) with constant stirring on magnetic stirrer at 4ºC overnight. Next morning, the bag was transferred into buffer II (300 mM NaCl, 10% glycerol and 50 mM Tris (pH7)) at 4ºC for 4 hours. The TEV cleaved protein was passed through HisTrap™ 5 ml column to remove the cut

6x His tag, GST tag and uncut protein and the flow through containing cleaved protein was collected. This was tested by running on the SDS-PAGE.

2.8 g) Protein concentration and estimation

The TEV cleaved protein was concentrated from 10 ml to 500 µl using amicon concentrator MWCO 3 kDa by centrifuging the protein at 3500 rpm at 4ºC. Dilutions were made (1:50, 1:100) by dissolving 1 µl of protein into 49 µl and 99 µl of 6M guanidine HCl respectively. Protein concentration was by Nick-Pace formula using A_{280} values and theoretical molar extinction coefficient (Ex-PASy-Protparam).
Protein concentration was also estimated using Bradford method. Series of known dilutions of BSA (Bovine serum albumin) was used to obtain a standard curve and the concentration for unknown protein was estimated using straight line equation.

2.8 h) Size Exclusion chromatography (SEC)

SEC was carried out to separate the proteins according to their size and molecular weight. The concentrated protein was injected into a HiLoad 16/60 Superdex S75 gel filtration chromatography column pre-equilibrated with SEC equilibration buffer (50 mM Tris pH7, 100 mM NaCl and 10% glycerol). The eluted peak fractions were collected at the rate of 1 ml/min and pooled based on the graph observed. The peak fractions eluted wererun on SDS-PAGE for analysis. The protein was then further concentrated again to 500 µl. The purified protein was the aliquoted in PCR tubes, flash frozen in liquid nitrogen and stored at -80ºC for later use.

2.8 i) SDS-PAGE analysis

SDS-PAGE, sodium dodecyl sulfate polyacrylamide gel electrophoresis, is an analytical technique which is used to separate proteins according to their molecular weight under denaturing conditions (Laemmli, 1970). SDS acts as an anionic detergent which denatures secondary and tertiary structures of protein and allows the protein to have overall negative charge. The protein samples were mixed with 4X protein loading dye containing 250 mM Tris-HCl pH 6.8, 10% SDS, 0.02% bromophenol blue, 5% β-merceptoethanol and 30% glycerol followed by boiling of samples at 90ºC for 5 minutes to break the disulphide bonds.The samples prepared

were run on 4-20% Tris-Glycine gradient and 12% gel using 1X running buffer containing 25 mM Tris, 192 mM Glycine and 0.1% SDS.at 100-110 V.

2.8 j) Western Blot analysis

The proteins samples were run on SDS- PAGE and transferred on the nitrocellulose membrane (NC) via wet transfer at 180 mA for 90 minutes using Bio-Rad apparatus. Blocking was done in blocking buffer (4 % BSA in 1X phosphate buffer saline (PBS)) for 1 hour at room temperature. Direct blot horseradish peroxidase (HRP) conjugated anti-His (Bio-legend) and anti-GST (Bio-legend) antibodies were diluted in the ratio of 1:10000 in 1x PBST buffer containing 4% BSA.The blots were kept for 2 hours incubation at room temperature for antibody bindingfollowed by three 1X PBST washes for 5 minutes each. Western blots were developed using DAB (3, 3'-diaminobenzidine) as chromogenic substrate in the presence of hydrogen peroxide (H_2O_2) in the dark room.

Western blottingwas also done using enhanced luminol-based chemiluminescent (ECL) substrate. Where, the proteins separated on the SDS-PAGE were transferred onto PVDF (polyvinylidene difluoride) membrane by wet transfer at 180 mA for 90 minutes. After transfer, the blots were blocked in 5% non-fat dry milk in TBS-T (20 mM Tris-HCL, 150 mM NaCl, 0.1% Tween-20) for 1 hour at room temperature. Primary and secondary antibodies were prepared with 2.5% non-fat dry milk in TBS-T. Membranes were incubated with primary antibody for overnight at 4ºC. The blots were further washed with TBS-T three times for 10 minutes each followed by incubation with HRP-conjugated secondary antibody for 1 hour at room temperature. Proteins were detected using ECL western blotting detection reagent kit (Bio-rad).

2.8 k) Crystallization

The protein was concentrated to 10mg/ml. Commercially available crystallisation screens I and II (Hampton Research) were used to set up the 96 -well flatbottomed plate. To the 96-well sitting drop plates, 150 nl sitting drop were set at three protein to buffer ratios (1:1, 1:2 and 2:1) using nanolitre liquid dispensing robot (Mosquito, TTP Labtech). The plate was then kept in the incubator set at temperature 20ºC and observed regularly.

CHAPTER 3

Results and Discussions

3.1 Optimisation of conditions for the expression of CNGC19 Cytosolic domains

The main aim of the study was to overexpress and purify the cytosolic domains of CNGC19 to elucidate the three-dimensional structure of AtCNGC19. In Arabidopsis, CNGC19 are tetrametric proteins having cytosolic N-terminal followed by C-terminal domain having two important binding domains (CNBD and CaMBD).The overexpression of cytosolic domains was carried out by performing small scale test expression experiments to optimise certain parameters like temperature, bacterial host strain, IPTG concentration, incubation period and buffers.

3.1.1 Selection of suitable bacterial strain for the expression of CNGC19 N-terminal domain

Characterisation of an unknown protein requires selection of an appropriate expression system. Protein expression was carried out largely by trial and error in *E. coli-based* bacterial expression system. N-terminal domain having 408 aa was expressed in two *E.coli* strains Rosetta2 (DE3) pLysS and BL21 (DE3) and optimised for best expression conditions. Small scale test expression was carried out using 0.4 mM IPTG followed by incubation at three different temperatures 20ºC, 25ºC and 37ºC. Cells were lysed using lysis buffer containing 50 mM Tris pH 7, 150 mM NaCl, 1 mM Benzamidine HCl, 1 mM PMSF, 2 mM $MgCl_2$, 10 µg/ml DNase-I and100 µg/ml Lysozyme. The expression of N-terminal was analysed from the samples collected (lysate, pellet, supernatant, flowthrough, washes and elution) during the process of protein purification through Nickel affinity bead binding.

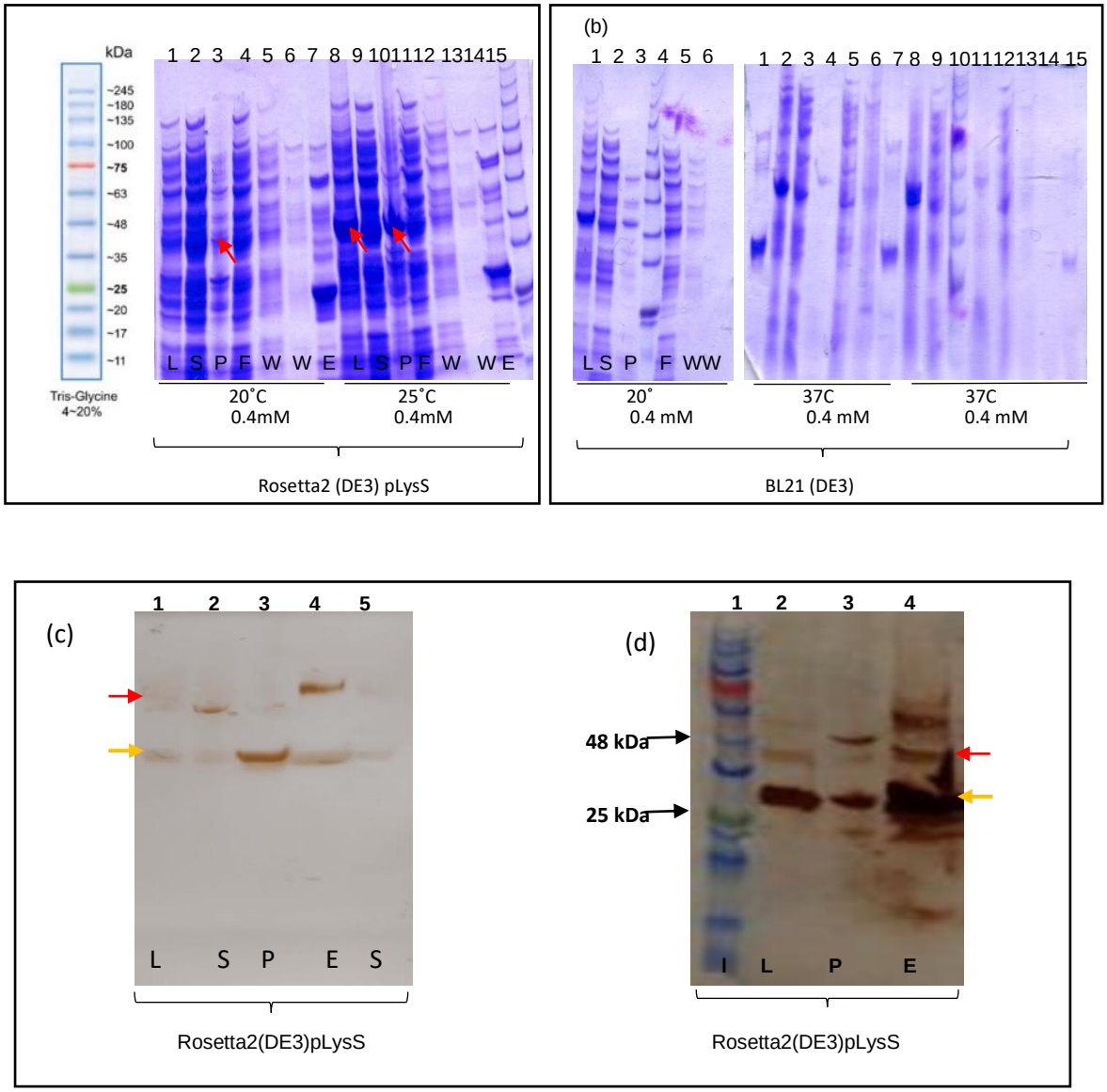

Figure 3.1: Small scale test expressionto optimise the bacterial strain for the expression of N-terminal in Rosetta2 (DE3) pLysS and BL21 (DE3) (a) Lanes-1 to 7 represents the expression of N-terminal in Rosetta2 (DE3) pLysS at 0.4 mM IPTG incubated at 20ºC and 25ºC where red arrow indicates the N-terminal His-tagged (46.4 kDa) protein in lysate and pellet. (b) The expression of N-terminal in BL21 (DE3) at 0.4 mM IPTG incubated at 20ºC, 25ºC and 37ºC. (c) and (d) Western blot developed against His-tagged antibody for the samples conditioned at 20ºC, 0.4 mM IPTG in Rosetta2 (DE3) pLysS confirms the presence of N-terminal domain in lysate, pellet, supernatant and elution as red arrows indicates N-terminal CNGC19 and yellow arrow indicates the enriched free GST (27 kDa). (L: Lysate, S: Supernatant, P: Pellet, F: Flow through, W: washes and E: elution).

Test expression experiments carried out in Rosetta2 (DE3) pLysS showed the presence of (46.4 kDa) His-tagged N-terminal protein at 20ºC, 0.4 mM IPTG. This was also confirmed by western blot analysis where red arrow indicates the presence of 46.4 kDa N-terminal protein and yellow arrows indicates free GST of size 27 kDa (Figure 3.1(c) and (d)). However, a large amount of protein was observed in pellet, which suggests that the amount of soluble protein present in the elution fraction is very low (Figure 3.1 (a) lane 10). The expression of N-terminal protein in BL21 (DE3) was not much conclusive (Figure 3.1 b) and no expression was observed. The expression of N-terminal in two different strains indicates that the use of engineered strains such as Rosetta™ can enhance the expression of heterologous protein significantly. Rosetta2 (DE3) pLysS strain solves the problem of codon optimization as it introduces rare codon tRNAs into the host cell and helps in easy expression of eukaryotic protein in prokaryotic bacteria.

3.1.2 Optimisation of IPTG concentration for the expression of CNGC19 N-terminal domain

The concentration of inducer used (IPTG) has major impact on the level of protein expression. Over-expression of protein using higher IPTG concentration might lead to partial folding of polypeptides which forms aggregates due to either non-covalent hydrophobic interactions or ionic interactions and gets accumulated as insoluble fractions in inclusion bodies (Villaverde et al., 2013). In order to obtain more amount of protein in soluble form, one of the approaches is to use suitable concentration of IPTG to minimize the possibility of protein going to inclusion bodies. To determine the optimal concentration of IPTG for the expression of N-terminal domain, small scale test experiments were performed in Rosetta2 (DE3) pLysS and BL21(DE3) using two different concentrations of IPTG i.e. 0.4 mM and 1 mM followed by incubation at 16˚C, 25˚C and 37˚C. Results obtained shows that in Rosetta2 (DE3) pLysS, production of N-terminal His tagged fusion protein at lower temperature i.e. 16˚C is almost negligible at both 0.4 mM and 1 mM as observed in Figure 3.2(a) lane 2-11. However, the lanes loaded with elution fraction shows the presence of enriched free GST marked with yellow arrows in lanes 6 and 11. Whereas the expression of protein at 25˚C and 37˚C indicates the presence of N-terminal His-tagged fusion protein band (46.4 kDa) only in the lanes loaded with pellet as observed in (Figure3.2 (a) lane 12, (b) lane 1, 7 and 12) marked with red arrows.

Western blot analysis of expression at 25ºC and 37ºC, also shows the presence of positive N-terminal His-tagged fusion protein band only in the pellet. However, lanes loaded with other fractions showed only enriched free GST bands.

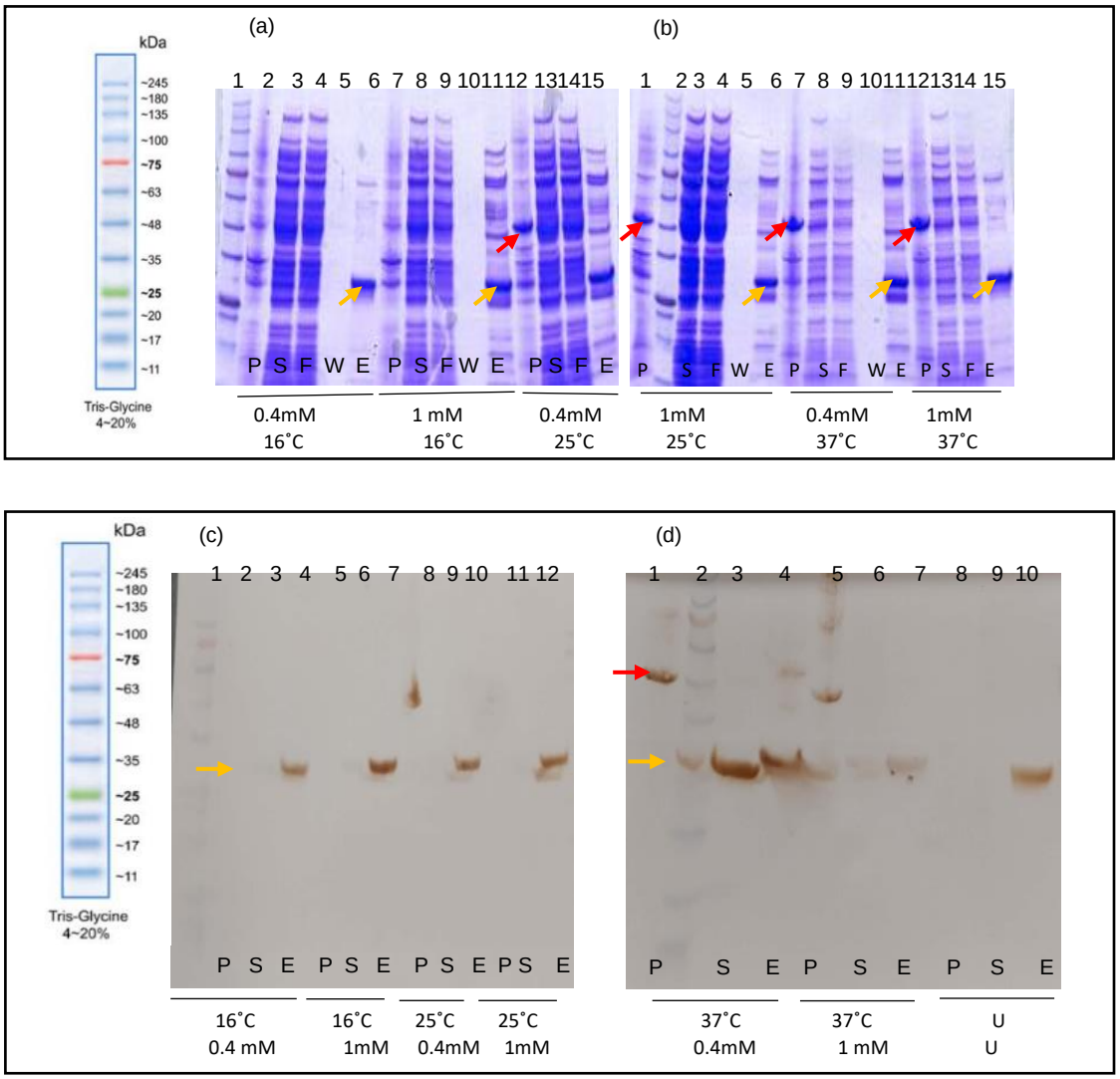

Figure 3.2 A: Small scale test expression to optimize IPTG concentration for the expression of N-terminal in Rosetta2 (DE3) pLysS (a) and (b) Represents the expression of N-terminal at 16º, 25º and 37ºC induced using 0.4 mM and 1 mM IPTG concentration where red arrows indicates the presence of N-terminal His-tagged fusion protein of size 46.4 kDa and yellow arrow indicates enriched GST (27 kDa) after batch binding. (c) and (d) Western blot developed against His-tagged antibody shows the expression of N-terminal (46.4 kDa) at both 25˚C and 37˚C in the pellet as observed in Figure (c) lane 8 and Figure (d) lane 1 and 5. However, less amount of protein was also observed in the eluted fraction at 0.4 mM, 37º

C Figure (d) lanes 4. (L: Lysate, P:Pellet, S:Supernatant, F:Flow through, W: washes and E: elution).

Small scale test expression was also performed in BL21 (DE3) using two different IPTG concentrations and shows that the production of N-terminal protein is more as compared to Roseta2 (DE3) pLys S indicated by red arrows Figure 3.2 (B). But, the amount of protein eluted after batch binding is very low and most of the protein is observed in pellet as insoluble fractions. Western blot analysis with His-tagged antibody for the same samples represents the N-terminal His-tagged fusion protein only in the lanes loaded with pellet Figure 3.2 B (d) lane 1, 5 and 11 (e) lane 1 and 5 marked with red arrows and none of the eluted fractions showed bands for fusion protein.

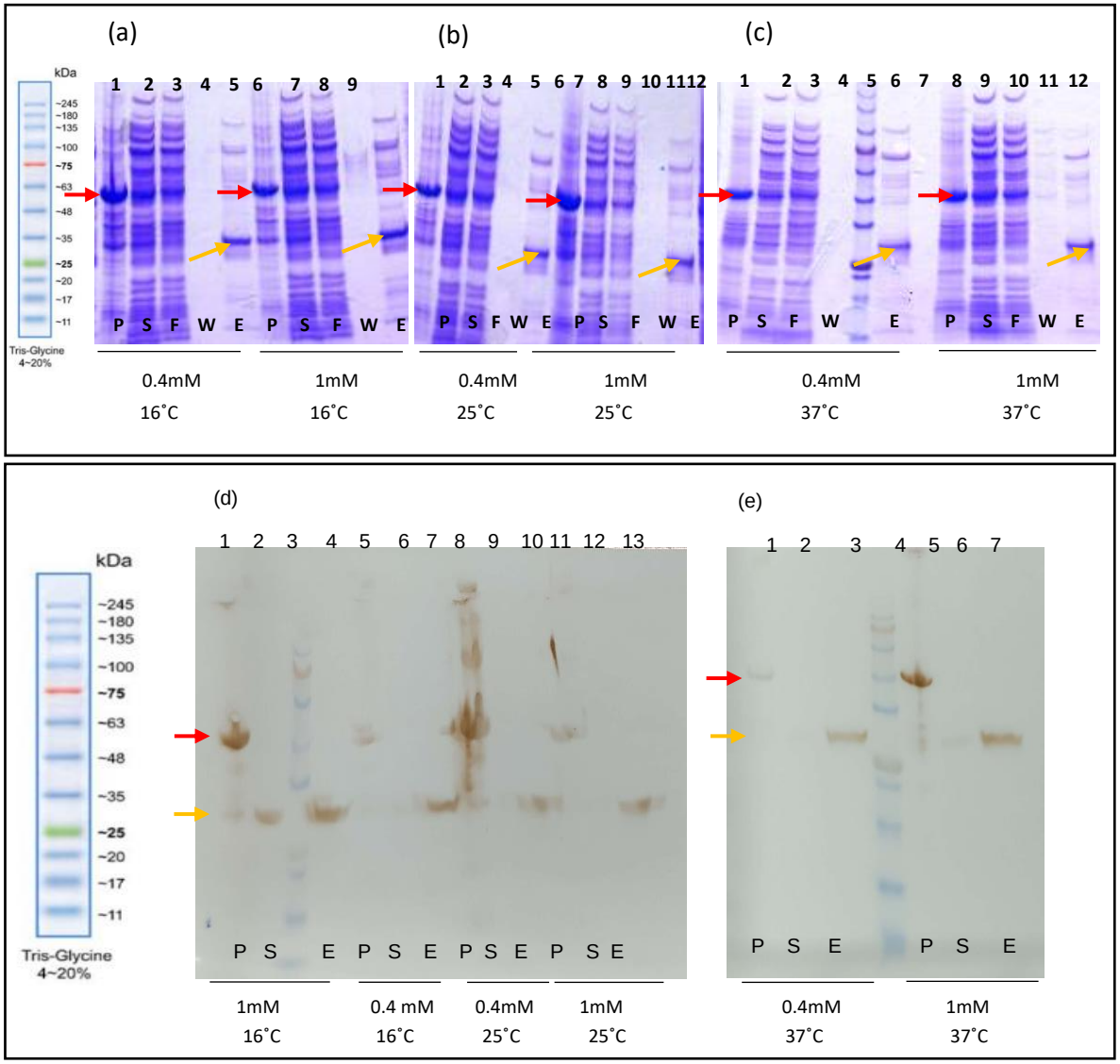

Figure 3.2 B: Small scale test expression to optimize IPTG concentration for the expression of N-terminal in BL21 (DE3):(a), (b) and (c) Represents the expression of N-terminal domain at 16º, 25º and 37ºC induced at two IPTG concentrations 0.4 mM and 1 mM where bands marked with red arrows indicates the N-terminal His-tagged fusion protein, while yellow shows the enriched free GST. (d) and (e) western blot with His-tagged antibody showing the expression in lysate, pellet, supernatant and elution samples collected. Bands for fusion protein of size 46.4 kDa was observed in the lanes loaded with pellet as observed in (c) lane 1, 5, 8 and 11 figure (d) lane 1 and 5 marked in red. Whereas, the positive band of size 27 kDa represents the free GST band marked in yellow. (L: Lysate, P: Pellet, S:Supernatant, F: Flow through, W: Washes and E: Elution).

High level of protein production upon induction with synthetic inducer such as IPTG effects the host fitness and associates a metabolic burden/load. This burden is attributed to the overconsumption of metabolic precursors such as amino acids, ATP, rRNAs to fuel the synthesis of foreign proteins or energy demanding maintenance of plasmid. IPTG added as an inducer leads to increase in the toxicity of substrate and causes significant damage to the *E. coli* host (Malakar and Venkatesh, 2012). Therefore, protein synthesis is optimised through evolution to maximise the growth of the bacteria and synthesise the desired protein in a particular environment minimising the cost by effectively tuning the concentration of IPTG to mitigate the negative effect (Larentis et al., 2014). It was observed that higher concentration of IPTG (1mM) and higher temperature incubation (25˚C and 37˚C) leads to increased rate of gene expression and therefore, resulting in more protein in pellet as insoluble fraction. Less concentration of IPTG (0.4mM) is optimal for soluble CNGC19 though it leads to low protein yield.

3.1.3 To optimise the lysis buffer for the optimal expression of N-terminal.

Various factors like the intrinsic nature of the protein, rate of gene expression, lack of molecular chaperones and many others contributes to the insolubility of the protein and formation of aggregation in the inclusion bodies (Marco et al., 2005). One of the approaches to solubilise such aggregation-prone protein from insoluble fraction is by using surfactants such as Triton-X-100. Heterologous protein production is not only affected by transcriptional activity but also by stability of the plasmid. Plasmid maintenance at high copy number imposes a metabolic burden on the cell that

reduces the overall production of heterologous protein. There are reports showing that the expression of unnecessary host proteins leads to the fractional reduction in growth rate and associate costs and burdens the cell. And this cost was reduced with the increase in glycerol concentration (Malakar and Venkatesh, 2012). In order to get more amount of soluble protein, small scale test expression was carried out in Rosetta2 (DE3) pLysS at 0.4 mM concentration of IPTG. Lysis was performed by using two kinds of lysis buffer LB- A containing 10% glycerol without Triton-X-100 and LB- B containing 10% glycerol with Triton-X-100 as detergent to ensure efficient lysis of cells.

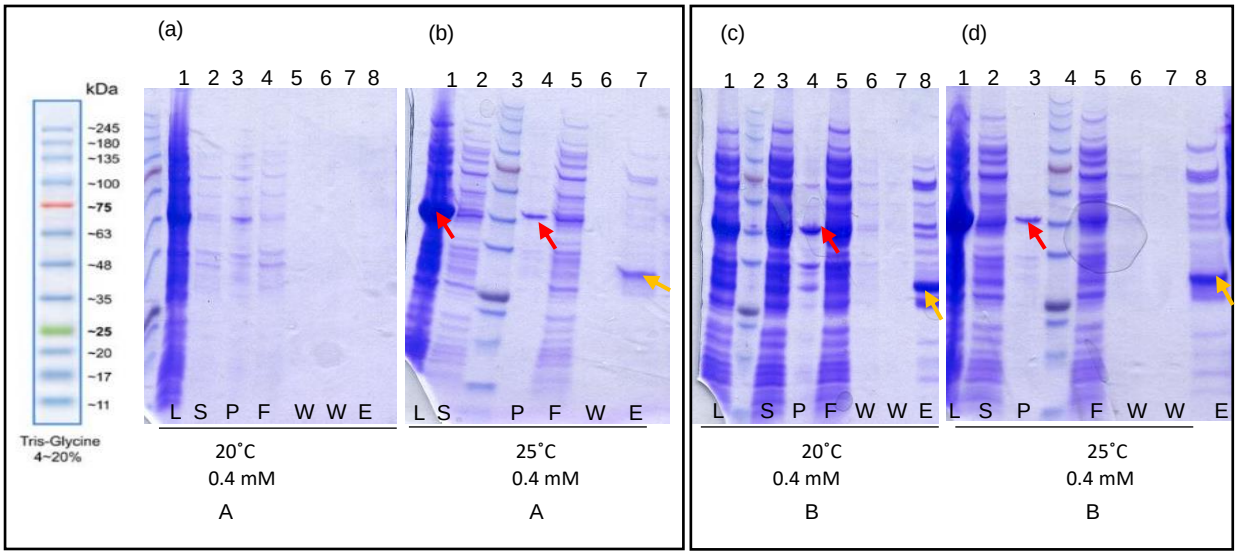

Figure 3.3 : Represents the expression of N-terminal in Rosetta2 (DE3) pLysS at 0.4 mM IPTG, incubated at 20ºC and 25ºC for the optimisation of lysis buffers. (a) and (b) Cell lysis using lysis buffer A containing 10% glycerol. (c) and (d) Cell lysis using lysis buffer B containing 10% glycerol and 1% Triton-X-100 as detergent. The presence of N-terminal His-tagged fusion protein are marked by red arrows and yellow arrows shows the free GST in the eluted fractions lane 8 (L: Lysate, P: Pellet, S: Supernatant, F: Flow through, W: Washes and E: Elution).

Results obtained show the difference in lysis pattern by using two lysis buffers. Presence of less amount of protein in the lanes loaded with supernatant and pellet figure (a) and (b) shows that cells lysed with Buffer A with no detergent, undergo partial lysis and fails to release the proteins into the supernatant. Whereas the cells

lysed with buffer B has 10% glycerol which acts as a co-solvent and thus, increases the stability of the proteins in aqueous solution by stabilising aggregation-prone intermediates and inhibiting protein unfolding (Vagenende et al., 2009). More stability of the protein in case B can also be due to the addition of Triton-x-100 that acts as a detergent. Triton-X-100 prevents hydrophobic membrane proteins from getting aggregated and their interaction with phospholipids thus, making the protein more soluble. Despite lysing the cells in the presence of detergent, membrane proteins continue to be integrated in lipid bilayers and associate with other proteins giving rise to large insoluble complexes which are observed as insoluble fraction in the samples loaded with pellet as Figure 3.3 (c) lane 4 and Figure 3.3 (d) lane 3. Apart from this, free GST bands are clearly visible in the eluted fractions marked with yellow arrows Figure 3.3. (c) and (d) lane 8 which suggest that protein synthesis under this condition led to the formation of truncated protein which could be due to the failure of codon optimisation where the bacterial strain fails to provide all the tRNAs required for the synthesis of entire protein.

3.1.4 To optimize the conditions for the expression of N-terminal

From the earlier performed test expressions, we observed that N-terminal was obtained in soluble form at one of the conditions which is 0.4 mM IPTG followed by incubation at 20ºC in Rosetta2 (DE3) pLysS which was also confirmed by western blot analysis Figure 3.1(d). The goal here was to express N-terminal at similar conditions again and then lyse the cells using two lysis buffer containing 10 % glycerol in the presence and absence of detergent i.e. Triton- X 100. The expression was tried at lower IPTG concentration (0.1 mM) so as to get more protein in soluble fraction. Small scale test experiments were performed to express N-terminal domain in Rosetta2 (DE3) pLysS at 0.4 mM and 0.1 mM concentration of IPTG followed by incubation at 20ºC and 25ºC and lysed using two kinds of lysis buffer- A containing only 10% glycerol and B containing 10% glycerol and 1% Triton-X-100.

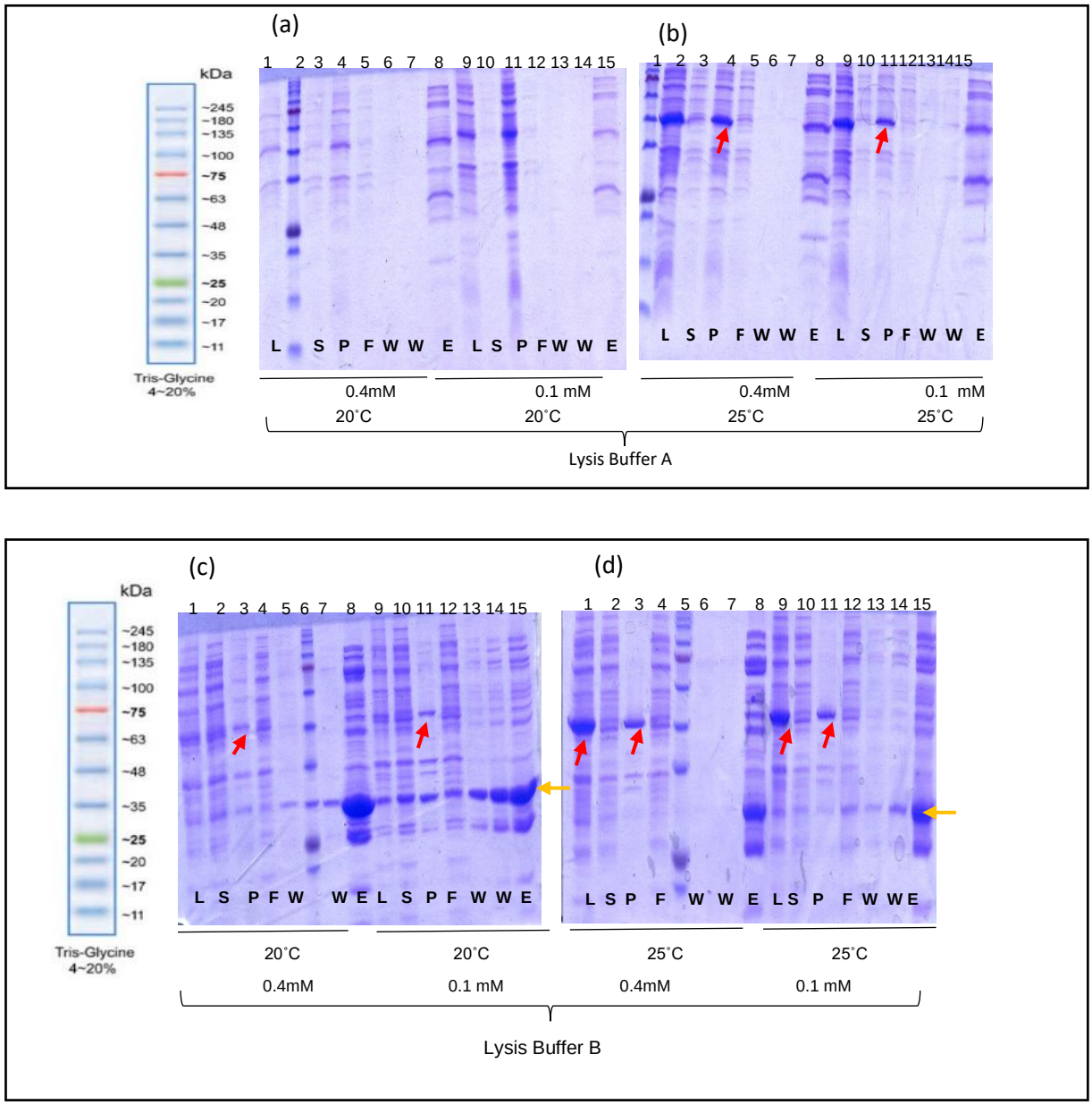

Figure 3.4: Small scale test expression of N-terminal in Rosetta2 (DE3) pLysS induced using 0.4 mM and 0.1 mM of IPTG (a) and (b) incubation at 20˚C and 25˚C respectively and lysed using Lysis buffer A. (c) and (d) Incubation at 20˚C and 25˚C respectively and lysed using Lysis buffer B. N-terminal His-tagged fusion protein was observed in pellet marked with red arrows and GST marked with yellow arrows. (L: Lysate, P: Pellet, S:Supernatant, F: Flow through, W: Washes and E: Elution).

The above small-scale test experiments for the expression of N-terminal under different conditions indicates that N-terminal is poorly expressed in soluble form. And out of all the tested conditions, only one of the conditions showed expression in

western blot where N-terminal was expressed in Rosetta2 (DE3) pLysS using 0.4 mM IPTG at 20ºC. SDS-PAGE and western blot analysis indicates the presence of more amount of protein in the pellet which indicates that a large fraction of protein tends to form insoluble aggregates and enters inclusion bodies. Apart from the N-terminal fusion protein of 46.4 kDa, SDS analysis also reveals the presence of truncated protein forms which is observed as free GST. The possible explanation for this could be the translation stalling and termination during protein biosynthesis resulting into the incomplete synthesis of N-terminal protein. Therefore, the expression of N-terminal domain needs further optimisation.

3.2 Optimisation of conditions for the expression of C-terminal domain

3.2.1 Optimisation of bacterial strain for the expression of C-terminal I

The expression of C-terminal domain was optimised using suitable *E.coli* strain. Small scale test experiments were performed to express C-terminal I in two strains - Rosetta2 (DE3) pLysS and BL21 (DE3) at 0.4 mM IPTG followed by incubation at 16˚C and 20˚C along with uninduced with no IPTG induction. Lysis was done using lysis buffer containing 50 mM Tris pH 7.4, 150 mM NaCl, 1 mM Benzamidine HCl,1% Triton-X 100, 10 % glycerol, 1 mM PMSF, 2 mM $MgCl_2$, 10 µg/ml DNase-I and 100 µg/ml Lysozyme.

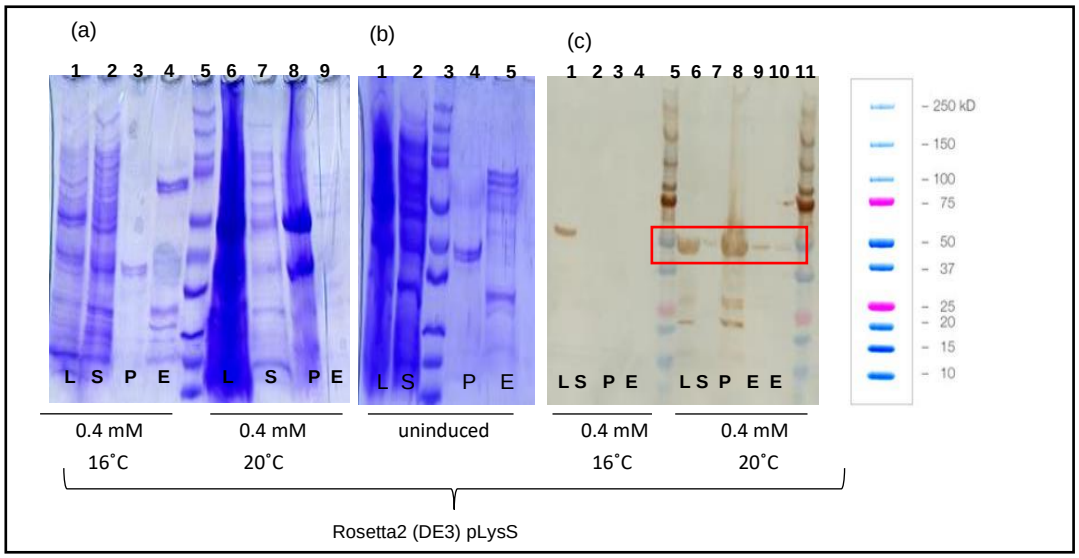

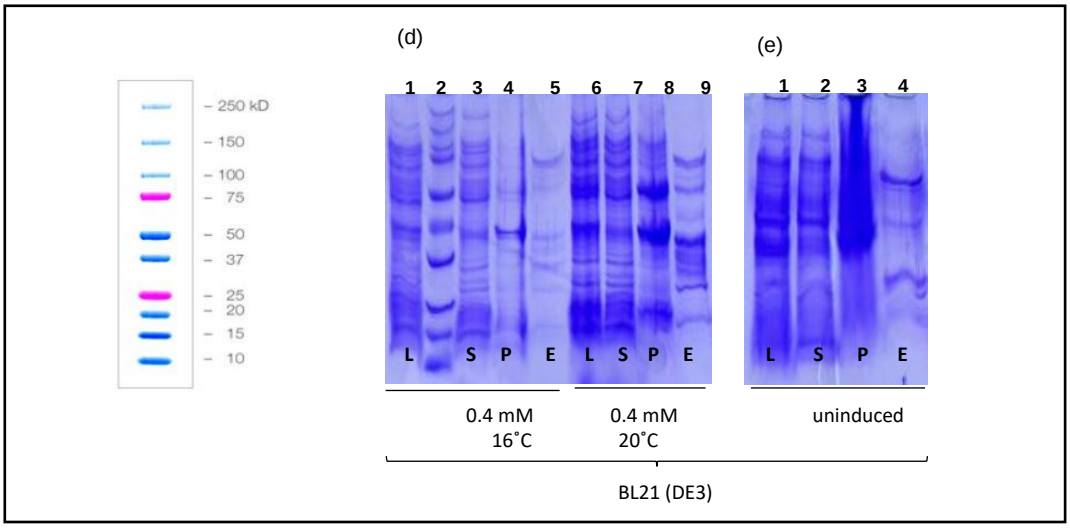

Figure 3.5: Small scale test experiments to optimize the suitable bacterial strain for the expression of C-terminal (a) Coomassie-stained SDS-PAGE gel representing the expression in Rosetta2 (DE3) pLysS at 16ºC and 20ºC induced using 0.4 mM of IPTG. (b) Expression of C-terminal in Rosetta2 (DE3) pLysS without IPTG induction (uninduced) : control (c) Western blot analysis against His-tagged antibody confirms the positive 52.4 kDa band for C-terminal His-tagged fusion protein, expressed at 20ºC,0.4 mM IPTG condition in Rosetta2 (DE3) pLysS in lysate, supernatant, pellet and eluted protein fraction as marked in red in lane 6-10. (d) Expression of C-terminal I in BL21 (DE3) at 16ºC and 20ºC using 0.4 mM IPTG concentration. (e) Control for expression of C-terminal in BL21 (DE3) without IPTG induction. (L: Lysate, S: Supernatant, P: Pellet, F: Flow through, W: Washes and E: Elution).

The above experiment shows that the expression of C-terminal domain was comparatively better in Rosetta2 (DE3) pLysS as compared to BL21 (DE3). The gel reveals the presence of 52.4 kDa His-tagged C-terminal I protein in one of the conditions where, the protein was expressed in Rosetta2 (DE3) pLysS at 20ºC, 0.4 mM IPTG. The obtained result was also confirmed by western blot analysis where lysate, supernatant, pellet and eluted protein fractions were loaded and western blotting was done against His-tagged antibody (Figure 3.5 (c) lane 6-10). However, the amount of protein observed in eluted fraction was much lower than the protein present in pellet which suggests that a large fraction of protein goes to pellet as insoluble fraction and the fraction coming out as soluble protein in eluted fraction is very low as labelled in red (c) lane 8,9 and 10 of Figure 3.5 (c). The presence of more amount of protein in pellet indicates the possibility of instability of the plasmid

resulting into the formation of protein aggregation and entering the inclusion bodies as insoluble fraction.

3.2.2 Optimisation of temperature for the expression of C-terminal I domain

The expression of C-terminal cytosolic domain was carried out in *E.coli* by optimising the temperature to maximise the amount of protein production in soluble form. C-terminal I domain having 452 aa was expressed in Rosetta2 (DE3) pLysS and optimised for best expression conditions. To optimise the suitable temperature for the expression of C-terminal domain, small scale test experiments were performed using 0.4 mM of IPTG concentration followed by incubation at three different temperatures 20ºC, 25ºC and 37ºC. Cell lysis was performed using lysis buffer containing 50 mM Tris pH 7.4, 150 mM NaCl, 1mM Benzamidine HCl, 1 mM PMSF, 2 mM $MgCl_2$, 10 µg/ml DNase-I and 100 µg/ml Lysozyme.

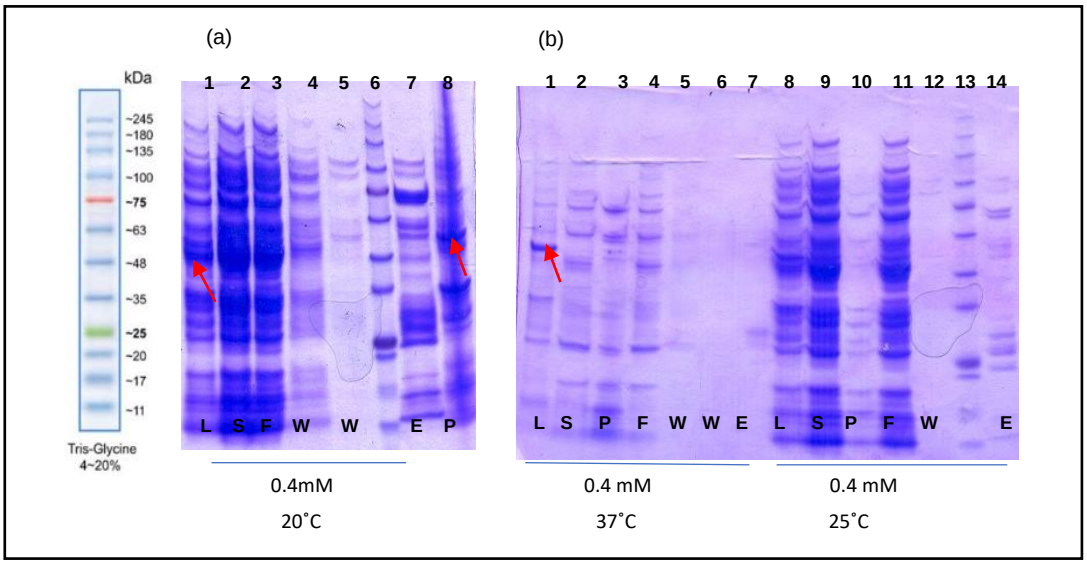

Figure 3.6: Represents the Coomassie gel for the expression of C-terminal induced using 0.4 mM IPTG at three different temperatures. (a) Expression at 20ºC, where red arrows indicate the 52.4 kDa C-terminal I protein in lanes 1, 2 and loaded with lysate, supernatant and pellet. (b) Expression at 25ºC and 37ºC (L: Lysate, P: Pellet, S: Supernatant, F: Flow through, W: Washes and E: Elution).

SDS analysis of the above experiment revealed that the expression of C-terminal was observed in Rosetta2 (DE3) pLysS at 20˚C using 0.4 mM IPTG. The presence of 52.4 kDa protein in the lanes loaded with lysate and pellet shows the

overexpression of C-terminal I protein Figure 3.6 (a) lane 1 and 8. However, the protein fails to be in supernatant and the eluted fractions collected after batch binding the suggests the loss of protein during purification. Whereas the protein expression at 25˚C and 37˚C shows poor expression of the protein. However, overexpression of the protein can be seen in the lanes loaded with lysate Figure 3.5 (a) lane 1 and (b) lane 1 as marked with red arrows.

3.2.3 Optimisation of IPTG concentration and incubation time for the expression of C-terminal I

From the earlier tested conditions, it was observed that temperature effects the production of protein and fails to keep the protein in soluble form. Thus, protein expression was tested together as a component of temperature, IPTG concentration used and the incubation time of the culture. To determine the suitable concentration of IPTG in order to obtain protein in soluble form, small scale test experiments were performed in Rosetta2 (DE3) pLysS using very low concentration of IPTG i.e. 0.25 mM at 20ºC but varying the incubation time period of the culture to 5 hours, 10 hours and 16 hours.

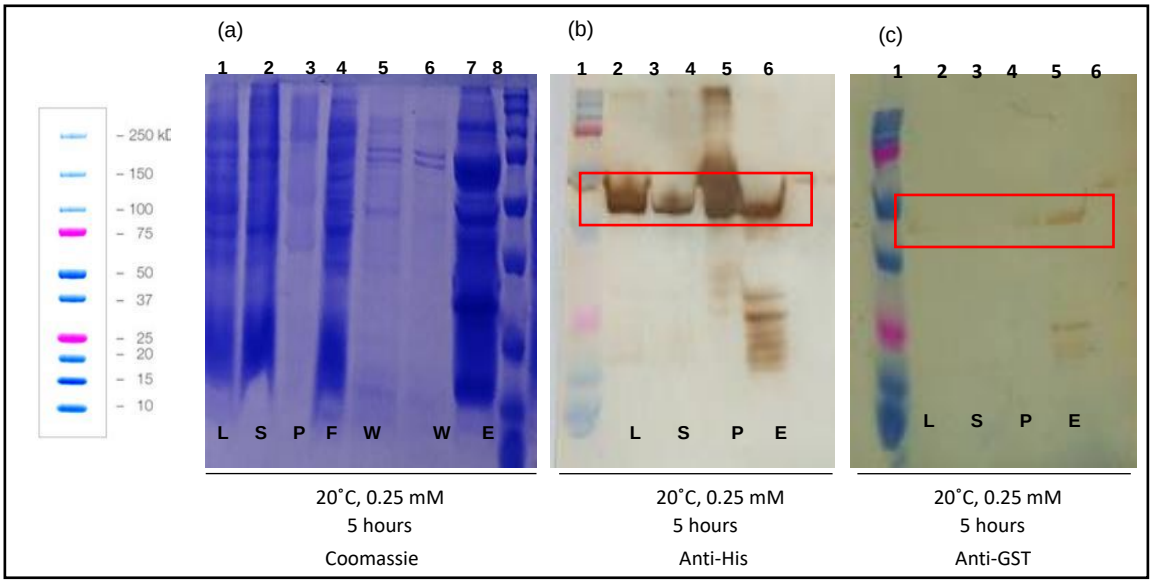

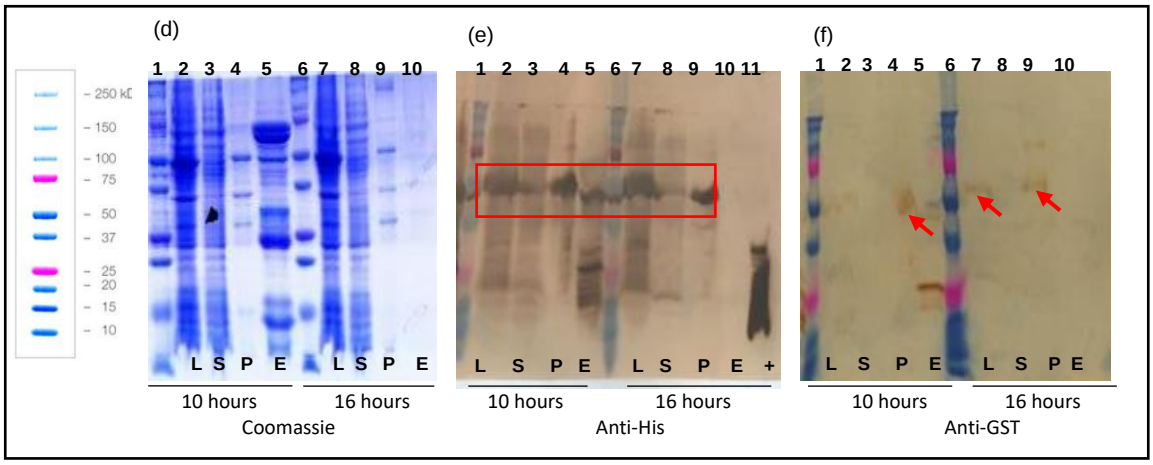

Figure 3.7: SDS-PAGE gels and western blot representing the expression of C-terminal I in Rosetta2 (DE3) pLysS using 0.25 mM of IPTG at 20ºC varying different incubation time periods. (a) Coomassie-stained 12% gel showing results for 5 hours. (b) and (c) Western blot analysis against anti-His and anti-GST confirming 52.4 kDa C-terminal protein in lane 2-6 loaded with samples conditioned at 5 hours incubation period as labelled in red colour.(d) Represents the expression of C-terminal at 10 hours from lane 1-5 and 16 hours from lane 7-10. (e) and (f) Western blot analysis using anti-His and anti-GST for the samples conditioned at 10 and 16 hours also confirms the 52.4 kDa C-terminal I protein in the lanes loaded with lysate, supernatant, pellet and elution as marked in red colour.

The above experiments revealed that IPTG concentration as well as incubation time period plays an important role in providing an optimal environment for the expression of any protein. The result obtained shows the variability in the behaviour of the protein at same IPTG concentration of 0.25 mM and temperature when kept under different incubation time period of 5, 10 and 16 hours. SDS analysis suggests that the protein expressed using 0.25 mM IPTG concentration for 5 hours at 20˚C shows better expression as compared to the protein expressed for longer incubation periods of 10 and 16 hours at same IPTG concentrationas seen in Figure 3.7 (b) and (e). This was confirmed with western blot showing 52.4 kDa C-terminal His-tagged fusion proteinband in lanes 2, 3, 4 and 5 loaded with lysate, supernatant, pellet and eluted protein fraction Figure 3.7 (b) and (c). Using lesser IPTG concentration means lesser toxicity for the cells which minimises the reduction in cell growth rate due to addition of IPTG as an inducer. Bacterial cell upon induction with IPTG starts synthesising protein but the cell resources such as availability of ribosomes often limits the productivity which appears as an additional burden for the cell and thus, the production of protein for prolonged period leads to more protein entering

inclusion bodies because of toxicity (Rosano and Ceccarelli, 2014). Better protein production at a lower IPTG concentration for much lower incubation time period gives us a clue that using lesser IPTG might result into higher possibility of obtaining protein in soluble form, so we tried to express C-terminal at much lower IPTG concentration.

3.2.4 Optimisation of C-terminal expression using low IPTG concentration

The small-scale experiments conducted earlier to express C-terminal I in Rosetta2 (DE3) pLysS by varying different conditions, it was observed that protein stability and solubility strictly depends on the concentration of IPTG used and temperature. Now, we tried to express C-terminal using very low IPTG concentration i.e. 0.05 mM at lower temperature (16ºC) but increasing the incubation time period to 3 days so as to slow down the transcriptional machinery resulting into the slow production and proper folding of protein in order to obtain more protein as soluble fraction.

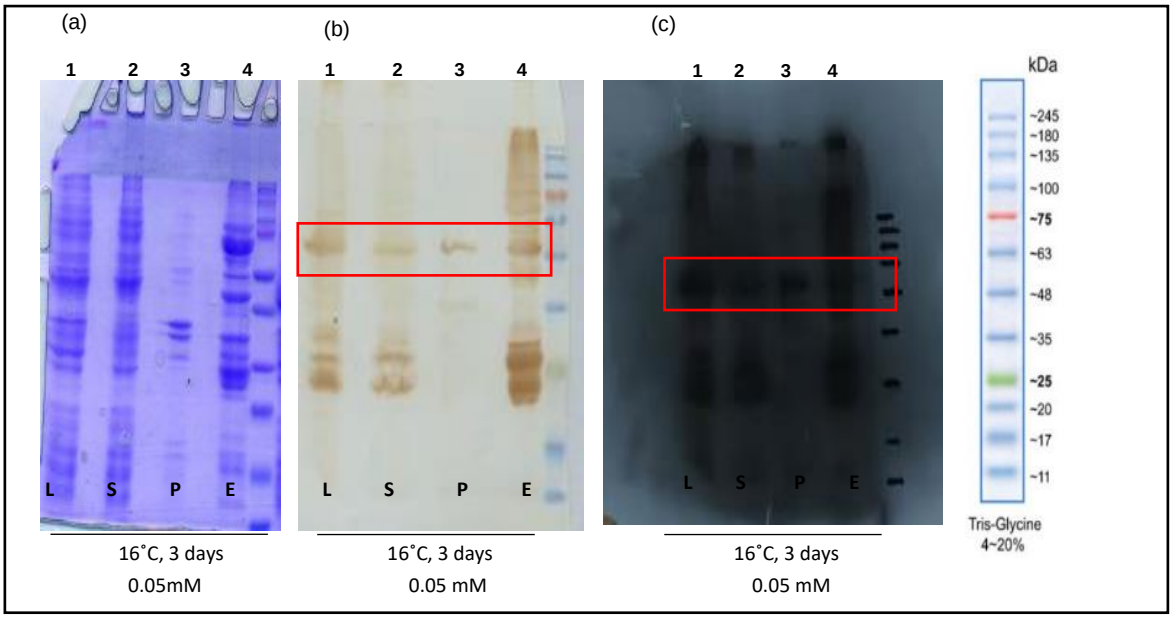

Figure 3.8: Small scale test expression of C-terminal I domain in Rosetta2 (DE3) pLysS using 0.05 mM IPTG at 16ºC for 3 days (a) Coomassie stained SDS-PAGE gel showing the expression 52.4 kDa C-terminal I protein in lanes 1-4 loaded with lysate, supernatant, pellet and elution. (b) Western blot against His antibody developed using DAB confirms the presence of C-terminal His-tagged fusion protein (52.4 kDa) in lane 1-4 as labelled in red colour. (c) Western blot against His antibody developed using ECL method with 30 seconds

exposure also confirms the results obtained by DAB labelled as red. (L: Lysate, P: Pellet, S: Supernatant, F: Flow through, W: Washes and E: Elution)

The expression of C-terminal I using very low IPTG concentration of 0.05 mM at much lower temperature (16ºC) but for longer incubation period resulted into the production of more protein in soluble form as observed in the lane 4 of Figure 3.9 (a) loaded with eluted fraction as marked with red arrows. The result obtained was confirmed using western blot analysis by both DAB development and ECL method and positive band for C-terminal I His-tagged protein band of size 52.4 kDa was observed in the lane loaded with elution by both the methods as labelled in red Figure 3.8 (b) and (c) lane 4. This suggests that lowering down the IPTG concentration and increasing the incubation time period increases the possibility of obtaining soluble protein. Thus, out of all the conditions tested in small scale experiments, this condition was selected to scale up the expression of C-terminal I domain.

3.2.5 Large scale overexpression of C-terminal I

The expression of C-terminal I was tested using different conditions by varying bacterial strain, temperature, IPTG concentration and incubation time period. One such condition was selected, and C-terminal was overexpressed on large-scale from 4 litres of bacterial culture (23.34 g of pellet) at much lower IPTG concentration (0.05 mM) at 16ºC for 3 days. The experiment was performed by transforming Rosetta2 (DE3) pLysS competent cells by heat shock method as mentioned in section 2.1 and further induced using 0.05 mM of IPTG concentration incubated at 16ºC for 3 days. Cell lysis was done as mentioned in section 2.1 using lysis buffer in the ratio of 1:5 and supernatant was collected and passed through the GE Ni-NTA column using peristaltic pump connected in loop at a very slow rate for overnight binding. Gradient elution was done using elution buffer containing 500 mM imidazole with fraction size of 3 ml. The graph obtained from AKTA after gradient elution showed two peaks. Based on this graph, peak fractions were collected and run on 12% gel Figure 3.9.

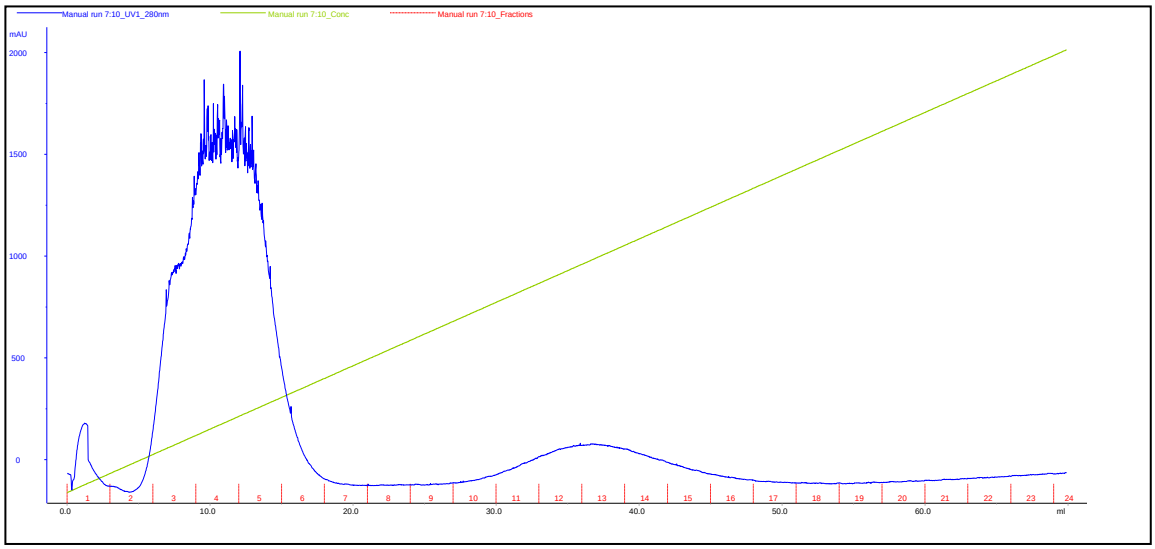

Figure 3.9: Protein purification of C-terminal I: Chromatogram showing the gradient elution after Ni-NTA affinity chromatography with fraction volume of 3ml.

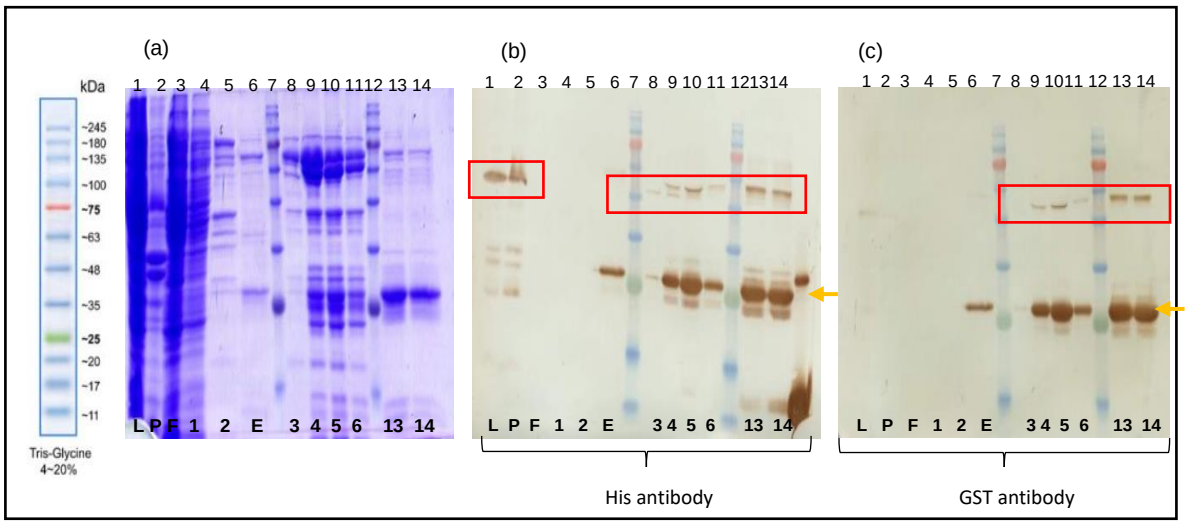

Figure 3.10: Coomassie-stained SDS-PAGE and western blot analysis for the fractions eluted after affinity chromatography (a) Lane 1: lysate, lane 2: pellet, lane 3: flow through, lane 4 and lane 5 contains 10 mM wash and 20 mM wash. Lane 6: EDTA wash, Lane 8-11 loaded with peak fractions 3, 4, 5 and 6. Lane, 12-14 loaded with peak fractions 13 and 14 showing 52.4 kDa C-terminal His-tagged fusion proteins. (b) Western blot of the same samples followed by DAB development against His antibody representing the fusion protein of size 52.4 kDa labelled as red. (c) Western blot with anti-GST antibody also showing the C-

terminal protein of size 52.4 kDa in the peak fractions. (L: Lysate, P: Pellet, S: Supernatant, F: Flow through, W: Washes and E: Elution)

It was observed that the peak fractions collected after affinity chromatography has very low level of protein production which was detected as faint bands in western blots both by anti-His and anti-GST antibody. The fractions collected from peak 1 showed C-terminal I protein bands of size 52.4 kDa as observed in coomassie in lane 8,9,10 and 11 (Figure 3.10 (b)). Western blot using His-tagged and anti-GST antibody confirmed the results. However, the amount of fusion protein detected was low. The protein estimated from the pooled fraction was 27.6 mg/ml. Free GST having size 27 kDa was highly enriched in the peak fractions eluted as observed in the western blot also. The fractions collected from peak 2 also showed positive bands after DAB development as observed in lane 12, 13 and 14 (Figure 3.11 (b)). Concentration of the pooled protein was estimated using UV_{280} absorbance and Bradford assay. TEV cleavage and dialysis was performed and then passed through the column, flow though was collected.

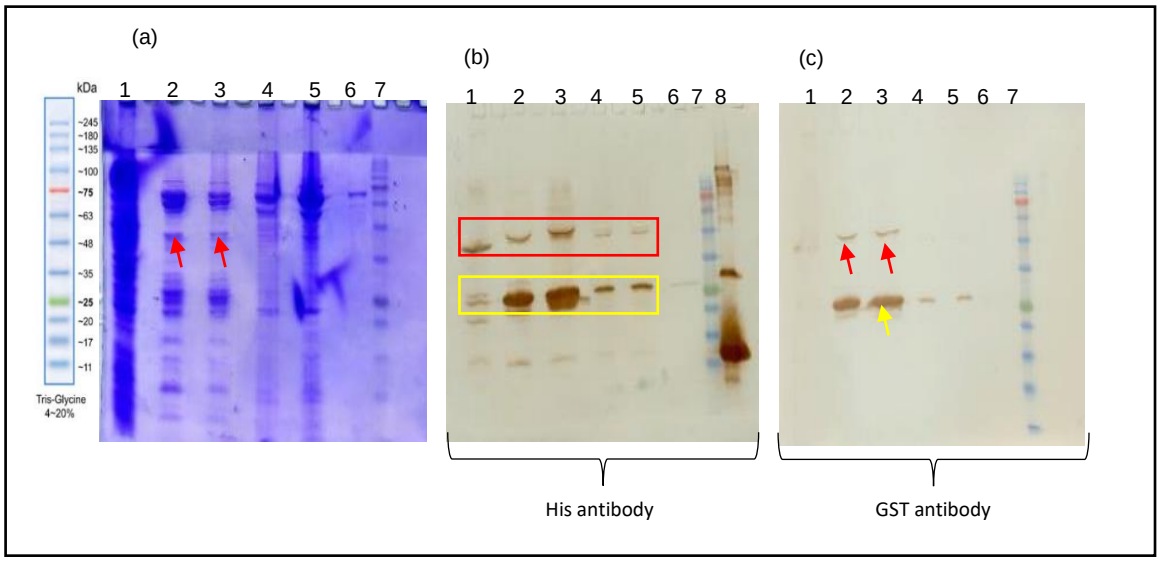

Figure 3.11: SDS-PAGE and western blot analysis of the purified C-terminal protein. (a) Coomassie-stained 12% gel of the purified protein after TEV cleavage and dialysis where Lane 1 represents the crude lysate, lane 2 represents the pooled uncut protein, lane 3 represents TEV cleaved protein, lane 4 and 5 represents the TEV cleaved concentrated protein and lane 6 represents the TEV cleaved protein after passing through His trap column. (b) Western blot analysis using His antibody shows positive bands of size 52.4 kDa

in lanes 1-5 labelled in red. (c) Western blot using anti-GST antibody also confirms the C-terminal protein.

SDS-PAGE and western blot analysis revealed that the production of C-terminal protein is low upon scaling up the volume, which was detected in western blots both by anti-His and anti-GST antibody. It was observed that there is very less difference between the pooled uncut protein and TEV cut protein as observed in lane 2 and 3 of Figure 3.11 (a) which suggests partial or insufficient cleavage of the His-tagged fused C-terminal protein as marked with red arrows. However, western blot for the cut and uncut showed partially cleaved protein as the amount of free GST observed is more in lane 3 than lane 2 marked in yellow Figure 3.11 (b). The presence of fusion protein bands in lane 4 and 5 indicates the fusion protein that remains uncut after TEV cleavage Figure 3.11 (b). One of the possible reasons for the low level of protein production could be the instability of the cytosolic domain independently and getting cleaved during the process of translation. Another factor could be the presence of cysteine residues which might lead to difficulty in expressing the protein having cysteines in heterologous system. Upon lysis, protein is exposed to oxidized environment where disulphide bonds are formed which could be rectified by adding reducing agents like DTT and β-merceptaethanol. Ribosomal jump and mid-way cleaving of N-terminal His-tags getting cleaved from C-terminal might also be responsible for the low yield of the protein.

3.3Optimisation of conditions for the expression of CaM2

3.3.1 Optimisation of IPTG concentration and temperature for the expression of CaM2

CaM2 binds with C terminal of CNGC19 and is postulated to gate the channel (Meena et al., 2019). CaM2 having 412 aa was expressed in Rosetta2 (DE3) pLysS and small-scale test experiment was performed to optimise suitable conditions such as temperature and IPTG concentration for best expression. A pilot experiment was carried out to express CaM2 in Rosetta2 (DE3) pLysS using very low IPTG concentration i.e. 0.05 mM at lower temperature (16ºC) for 3 days. Cell lysis was performed using lysis buffer in the ratio of 1:10 ratio containing 50 mM Tris pH 7.4,

150 mM NaCl, 1 mM Benzamidine HCl,1 % Triton-X 100, 10 % glycerol, 1 mM PMSF, 2 mM $MgCl_2$, 10 µg/ml DNase-I and100 µg/ml Lysozyme, 100 mg/l Sodium cholate and 10 mM DTT.

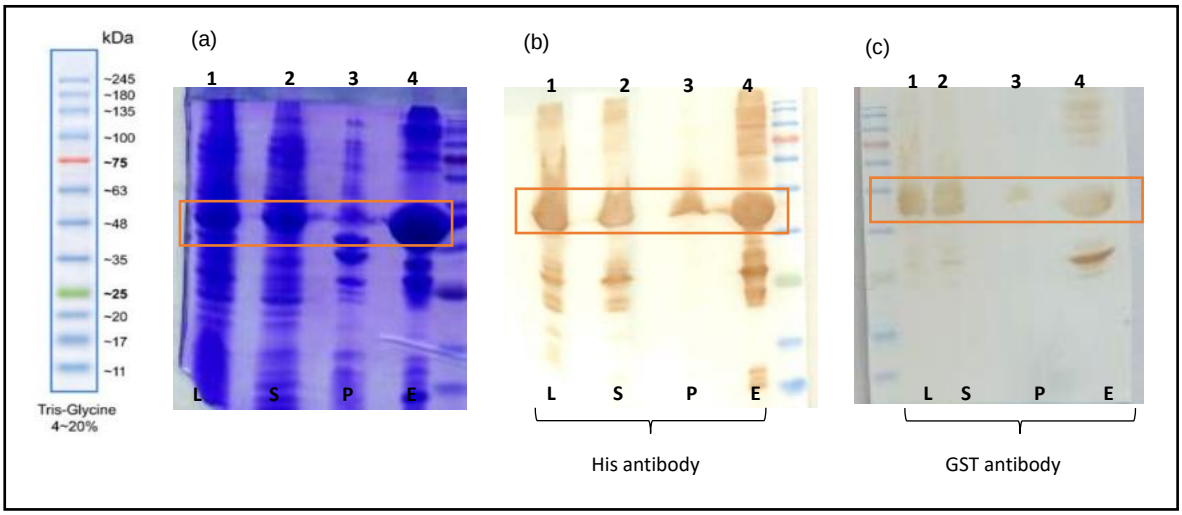

Figure 3.12: Small scale test expression of CaM2 (a) Coomassie-stained gel for CaM2 expression having size 47.0 kDa was observed in the lanes 1, 2, 3 and 4 loaded with lysate, supernatant, pellet and elution respectively. (b) Western blot developed by using DAB with HRP conjugated His-tagged antibody confirms the presence of CaM2 protein production in the given samples. (c) Western blot with HRP conjugated GST antibody also shows positive bands for CaM2 protein with DAB. Positive bands showing CaM2 protein of size 47.0 kDa is labelled within red.(L: Lysate, P: Pellet, S: Supernatant, and E: elution)

The above performed experiment shows that the CaM2 protein was successfully expressed and purified under the above-mentioned parameters. SDS gel analysis for His-tagged CaM2 protein depicts the protein band of size 47.0 kDa in lanes 1, 2, 3 and 4 loaded with lysate, supernatant, pellet and elution as marked in red colour. The obtained result was also confirmed by western blot where the samples were checked against His-tagged antibody Figure 3.12 (b) and GST antibody Figure 3.12 (c). This condition was selected for the large-scale over-expression of CaM2.

3.2 Large scale over expression of CaM2

On the basis of results obtained in small scale test expression of CaM2 in section 3.3.1, CaM2 was overexpressed on large scale from 1.6 litres of bacterial culture

(12.5g of pellet). CaM2 having size 47 kDa was overexpressed using similar conditions. Rosetta2 (DE3) pLysS competent cells were transformed using heat shock method as mentioned in 2.1 and induced using 0.05 mM of IPTG concentration followed by incubation at 16ºC for longer time i.e. 3 days. Cell lysis was done and the supernatant collected after lysis was passed through the GE Ni-NTA column using peristaltic pump connected in loop for binding and gradient elution was done using buffer containing 500 mM imidazole. Gradient elution was performed using AKTA, and peak fractions were collected on the basis of the obtained graph shown in Figure 3.14. The peak fractions having fraction size of 1 ml were collected and loaded on 12% gel.

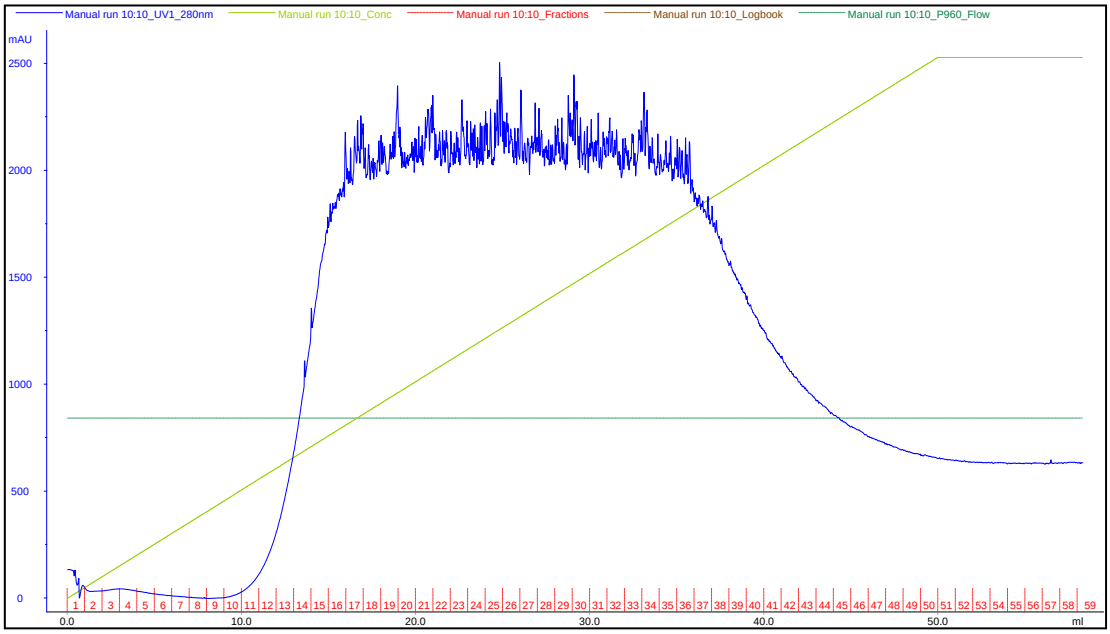

Figure 3.13: Chromatogram representing the gradient elution of CaM2 after Ni-NTA affinity chromatography.

The fractions were collected from fraction number 13- 40 of having fraction size of 1 ml were collected and pooled down to 27 ml of protein. SDS-PAGE gel analysis shows a good yield of CaM2 protein production in the peak fractions collected after gradient elution as observed in lane 1-8 in Figure 3.13 (a).

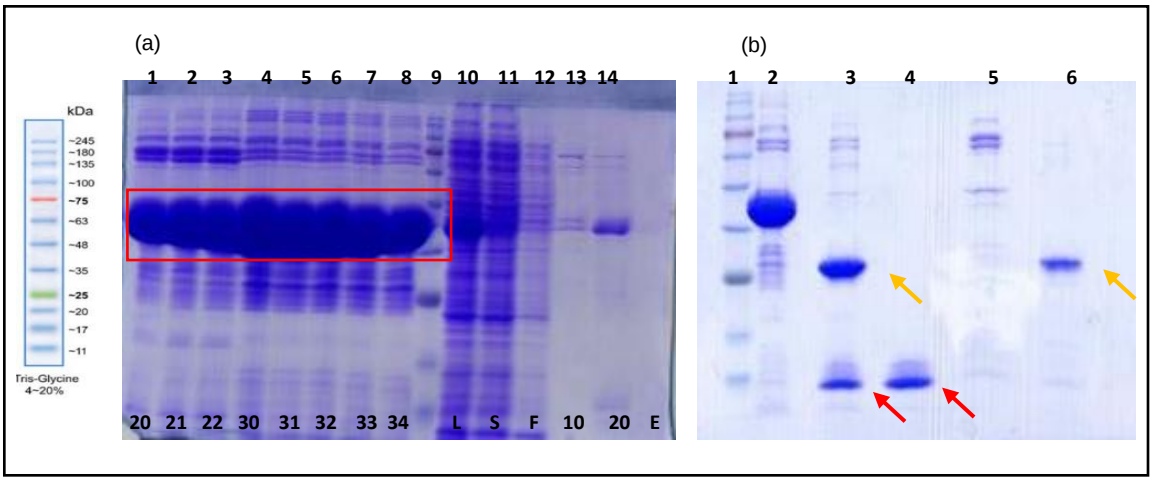

Figure 3.14 (a) Coomassie-stained SDS-PAGE gel for the fractions collected on the basis of graph obtained after affinity chromatography. Lane 1- 8 represents the peak fraction 20, 21, 22, 30, 31, 32, 33 and 34 collected followed by ladder. Lane 10 represents lysate. Lane 11 shows supernatant, lane 12 flow through, lane 13 was loaded with 10 mM wash, lane 14 contains 20 mM wash and lane 15 represents eluted protein with 500 mM imidazole containing elution buffer. (b) Coomassie-stained SDS-PAGE gel showing 1-pooled protein, 2-TEV cleaved protein showing GST of size 27 kDa and CaM2 protein of size protein less than 17 kDa labelled with yellow and red arrows respectively, 3- TEV cleaved protein after passing through column only showing CaM2, 4- column wash and 5- elution with 500 mM imidazole showing GST band marked in yellow. (L: Lysate, P: Pellet, S: Supernatant, and E: elution)

Concentration of the pooled fraction was estimated using UV_{280} absorbance. TEV cleavage and dialysis was performed as mentioned in methods section 2.8 (f). The TEV cleaved protein obtained was then passed through recharged His column and flow through was collected. The gel analysis of the purified protein after TEV cleavage and dialysis shows the cleaved CaM2 protein of size less than 17 kDa marked with red arrows and GST fragment of 27 kDa marked with yellow arrows Figure 3.14 (b). The concentration of the protein was estimated and further concentrated to 500 µl for size exclusion chromatography.

Sno.	Sample	Protein Concentration
1	Pooled protein fractions	121.5 mg/ml
2	TEV cleaved protein	32.92 mg/ml
3	Concentrated protein	26.87 mg/ml

Table 3.1: CaM2 protein estimation at various stages using Bradford's method.

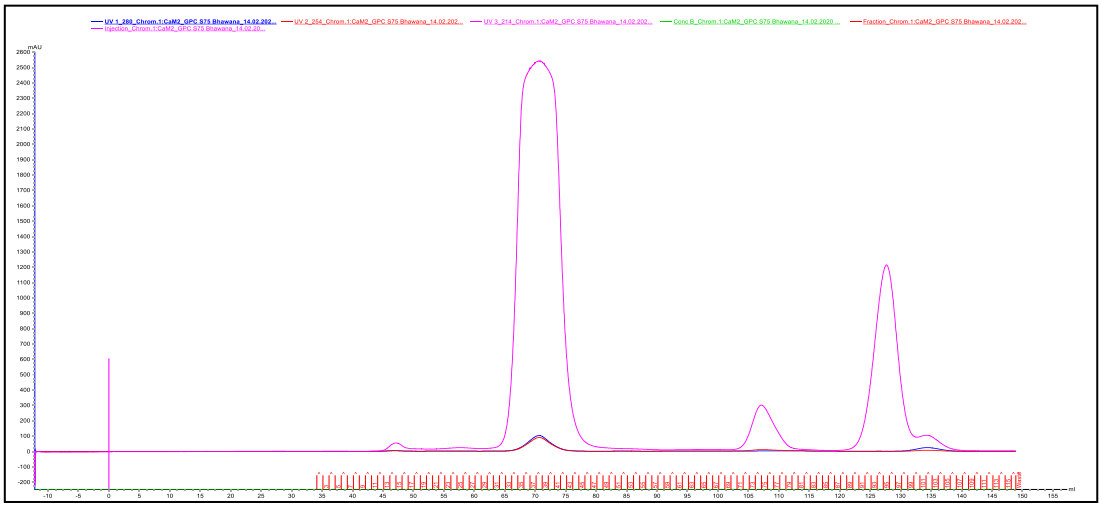

Figure 3.15. Chromatogram showing the GPC purified CaM2 protein using Superdex S75 column having fraction size of 1ml.

The concentrated protein was injected into Highload 16/60 Superdex S75 column pre-equilibrated with buffer containing 100 mM NaCl, 50 mM Tris pH 7.4, 10% glycerol and fractions were collected having fraction volume 1 ml. The SEC chromatogram obtained is shown in Figure 3.15. The peak fractions were pooled and further concentrated to 200 µl to set up crystallization

Crystallization of CaM2:

Crystal screens I and II (Hampton Research) were used to set up the 96-well flat-bottomed plate using liquid handling robot (Mosquito, TTP Labtech). The plate was incubated at 20ºC and observed regularly. Optimization of initial conditions to obtain diffraction quality crystals is under progress.

CHAPTER 4

Conclusions

CNGC19 is an important calcium channel involved in herbivory against Spodoptera attack in Arabidopsis. The aim of the project is to overexpress and purify the cytosolic domains of the calcium channel CNGC19. The (N-terminal and C-terminal) cytosolic domains of CNGC19 were cloned and small-scale test experiments were performed for over-expression by optimising various parameters like temperature, bacterial strain, IPTG concentration and buffers. Test expression in *E. coli* Rosetta 2 (DE3) pLysS has resulted in lead-conditions for large scale expression.

Test scale expression of N-terminal domain suggests that this domain is poorly expressed in soluble form. Out of all the screened conditions, N-terminal was expressed in Rosetta2 (DE3) pLysS using 0.4 mM of IPTG at 20ºC. However, a large fraction of protein tends to form insoluble aggregates due to either non-covalent hydrophobic interactions or ionic interactions and gets accumulated as insoluble fractions in inclusion bodies. N-terminal domain being closer to the membrane may be the reason for poor expression. The C-terminal domain was cloned and successfully expressed in Rosetta2 (DE3) pLysS and of all conditions tested 0.05 mM IPTG at 16ºC for 3 days resulted in best expression. A large-scale protein purification was set up for C-terminal domain and the yield of the protein has to be improved further for crystallization. N-and C-terminal domain of neighbouring ion channel subunits in the oligomer (tetramer) interact with each other, as evident from the existing cryo-EM structures from animals (Martinez and Gordon, 2019). Hence co-expression of these domains together may also result in improved yield. CaM2 was successfully cloned, expressed and purified by optimising various conditions. Expression in Rosetta2 (DE3) pLysS using 0.05 mM IPTG at 16ºC for 3 days yielded good pure protein for crystallisation. Extensive crystallisation trials with different concentrations and conditions are in progress. Expression of CNGC19 cytosolic domains and purification would help in determining the full-length structure of AtCNGC19 using X-ray crystallography and cryo-EM.

REFERENCES

Aljbory, Z., and Chen, M.S. (2018). Indirect plant defense against insect herbivores: a review. Insect Sci. *25*, 2–23.

Balagué, C., Lin, B., Alcon, C., Flottes, G., Malmström, S., Köhler, C., Neuhaus, G., Pelletier, G., Gaymard, F., and Roby, D. (2003). Plant Cell. *15*, 365–379.

Bari, R., and Jones, J.D.G. (2009). Role of plant hormones in plant defence responses. Plant Mol. Biol. *69*, 473–488.

Borsics, T., Webb, D., Andeme-Ondzighi, C., Staehelin, L.A., and Christopher, D.A. (2007). The cyclic nucleotide-gated calmodulin-binding channel AtCNGC10 localizes to the plasma membrane and influences numerous growth responses and starch accumulation in Arabidopsis thaliana. Planta *225*, 563–573.

Browning, D.F., Godfrey, R.E., Richards, K.L., Robinson, C., and Busby, S.J.W. (2019). Exploitation of the Escherichia coli lac operon promoter for controlled recombinant protein production. Biochem. Soc. Trans. *47*, 755–763.

Burgess-Brown, N.A., Sharma, S., Sobott, F., Loenarz, C., Oppermann, U., and Gileadi, O. (2008). Codon optimization can improve expression of human genes in Escherichia coli: A multi-gene study. Protein Expr. Purif. *59*, 94–102.

Charpentier, M., Sun, J., Martins, T.V., Radhakrishnan, G. V, Findlay, K., Soumpourou, E., Thouin, J., Véry, A., Sanders, D., Morris, R.J., et al. (2016). Symbiotic Calcium Oscillations. Science (80-.). *352*, 1102–1105.

Chen, R. (2012). Bacterial expression systems for recombinant protein production: E. coli and beyond. Biotechnol. Adv. *30*, 1102–1107.

Chiasson, D.M., Haage, K., Sollweck, K., Brachmann, A., Dietrich, P., and Parniske, M. (2017). A quantitative hypermorphic CNGC allele confers ectopic calcium flux and impairs cellular development. Elife *6*, 1–15.

Chin, K., Defalco, T.A., Moeder, W., and Yoshioka, K. (2013). The arabidopsis cyclic nucleotide-gated ion channels AtCNGC2 and AtCNGC4 work in the same signaling pathway to regulate pathogen defense and floral transition. Plant Physiol. *163*, 611–624.

Clough, S.J., Fengler, K.A., Yu, I.C., Lippok, B., Smith, R.K., and Bent, A.F. (2000). The Arabidopsis dnd1 “defense, no death” gene encodes a mutated cyclic nucleotide-gated ion channel. Proc. Natl. Acad. Sci. U. S. A. *97*, 9323–9328.

Cui, H., Tsuda, K., and Parker, J.E. (2015). Effector-Triggered Immunity: From Pathogen Perception to Robust Defense. Annu. Rev. Plant Biol. *66*, 487–511.

DeFalco, T.A., Marshall, C.B., Munro, K., Kang, H.G., Moeder, W., Ikura, M., Snedden, W.A., and Yoshioka, K. (2016). Multiple calmodulin-binding sites positively and negatively regulate arabidopsis CYCLIC NUCLEOTIDE-GATED CHANNEL12. Plant Cell *28*, 1738–1751.

Dodds, P.N., and Rathjen, J.P. (2010). Plant immunity: Towards an integrated view

of plantğ€" pathogen interactions. Nat. Rev. Genet. *11*, 539–548.

Edel, K.H., Marchadier, E., Brownlee, C., Kudla, J., and Hetherington, A.M. (2017). The Evolution of Calcium-Based Signalling in Plants. Curr. Biol. *27*, R667–R679.

Erb, M., and Reymond, P. (2019). Molecular Interactions Between Plants and Insect Herbivores. Annu. Rev. Plant Biol. *70*, 527–557.

Fernandes, I.P.G., and Oliveira-brett, A.M. (2017). Bioelectrochemistry Calcium-induced calmodulin conformational change . Electrochemical evaluation. Bioelectrochemistry *113*, 69–78.

Finka, A., Cuendet, A.F.H., Maathuis, F.J.M., Saidi, Y., and Goloubinoff, P. (2012). Plasma membrane cyclic nucleotide gated calcium channels control land plant thermal sensing and acquired thermotolerance. Plant Cell *24*, 3333–3348.

Fischer, C., Kugler, A., Hoth, S., and Dietrich, P. (2013). An IQ domain mediates the interaction with calmodulin in a plant cyclic nucleotide-gated channel. Plant Cell Physiol. *54*, 573–584.

Fischer, C., Defalco, T.A., Karia, P., Snedden, W.A., Moeder, W., Yoshioka, K., and Dietrich, P. (2017). Calmodulin as a Ca 2 + -Sensing Subunit of Arabidopsis Cyclic Nucleotide-Gated Channel Complexes Special Focus Issue – Regular Paper. *58*, 1208–1221.

Grunwald, M.E., Yu, W.P., Yu, H.H., and Yau, K.W. (1998). Identification of a domain on the β-subunit of the rod cGMP-gated cation channel that mediates inhibition by calcium-calmodulin. J. Biol. Chem. *273*, 9148–9157.

Hepler, P.K. (2005). Calcium: A central regulator of plant growth and development. Plant Cell *17*, 2142–2155.

Hou, S., Liu, Z., Shen, H., and Wu, D. (2019). Damage-associated molecular pattern-triggered immunity in plants. Front. Plant Sci. *10*.

Huang, M., Bao, J., and Nielsen, J. (2014). Biopharmaceutical protein production by Saccharomyces cerevisiae : current state and future prospects . Pharm. Bioprocess. *2*, 167–182.

Hunter, M., Yuan, P., Vavilala, D., and Fox, M. (2019). Optimization of Protein Expression in Mammalian Cells. Curr. Protoc. Protein Sci. *95*, 1–28.

Jammes, F., Hu, H.C., Villiers, F., Bouten, R., and Kwak, J.M. (2011). Calcium-permeable channels in plant cells. FEBS J. *278*, 4262–4276.

Jogawat, A., Meena, M.K., Kundu, A., Varma, M., and Vadassery, J. (2020). Calcium channel CNGC19 mediates basal defense signaling to regulate colonization by Piriformospora indica on Arabidopsis roots. J. Exp. Bot.

Jones, J.D.G., D.J.L. (2006). H E P L a N T Imm U N E S Y S T. *444*, 323–329.

Jurkowski, G.I., Smith, R.K., Yu, I.C., Ham, J.H., Sharma, S.B., Klessig, D.F., Fengler, K.A., and Bent, A.F. (2004). Arabidopsis DND2, a second cyclic nucleotide-gated ion channel gene for which mutation causes the “defense, no death” phenotype. Mol. Plant-Microbe Interact. *17*, 511–520.

Karban, R., and Myers, J.H. (1989). Induced plant responses to herbivory. Annu.

Rev. Ecol. Syst. Vol. 20 *20*, 331–348.

Kaupp, U.B., and Seifert, R. (2020). Cyclic Nucleotide-Gated Ion Channels. 769–824.

Kazan, K., and Lyons, R. (2014). Intervention of phytohormone pathways by pathogen effectors. Plant Cell *26*, 2285–2309.

Kiep, V., Vadassery, J., Lattke, J., Maaß, J.P., Boland, W., Peiter, E., and Mithöfer, A. (2015a). Systemic cytosolic Ca2+ elevation is activated upon wounding and herbivory in Arabidopsis. New Phytol. *207*, 996–1004.

Kiep, V., Vadassery, J., Lattke, J., Maaß, J.P., Boland, W., Peiter, E., and Mithöfer, A. (2015b). Systemic cytosolic Ca^{2+} elevation is activated upon wounding and herbivory in Arabidopsis. New Phytol. *207*, 996–1004.

Köhler, C., and Neuhaus, G. (2000). Characterisation of calmodulin binding to cyclic nucleotide-gated ion channels from Arabidopsis thaliana. FEBS Lett. *471*, 133–136.

Ladwig, F., Dahlke, R.I., Stührwohldt, N., Hartmann, J., Harter, K., and Sauter, M. (2015). Phytosulfokine regulates growth in arabidopsis through a response module at the plasma membrane that includes cyclic nucleotide-gated channel17, H+-ATPase, and BAK1. Plant Cell *27*, 1718–1729.

Larentis, A.L., Nicolau, J.F.M.Q., Esteves, G.D.S., Vareschini, D.T., De Almeida, F.V.R., Dos Reis, M.G., Galler, R., and Medeiros, M.A. (2014). Evaluation of pre-induction temperature, cell growth at induction and IPTG concentration on the expression of a leptospiral protein in E. coli using shaking flasks and microbioreactor. BMC Res. Notes *7*, 1–13.

Maffei, M., Bossi, S., Spiteller, D., Mithöfer, A., and Boland, W. (2004). Effects of feeding Spodoptera littoralis on Lima bean leaves. I. Membrane potentials, intracellular calcium variations, oral secretions, and regurgitate components. Plant Physiol. *134*, 1752–1762.

Malakar, P., and Venkatesh, K. V. (2012). Effect of substrate and IPTG concentrations on the burden to growth of Escherichia coli on glycerol due to the expression of Lac proteins. Appl. Microbiol. Biotechnol. *93*, 2543–2549.

Marco, A. De, Vigh, L., Diamant, S., and Goloubinoff, P. (2005). Ario de Marco, 1 Laszlo Vigh, 2 Sophia Diamant, 3 and Pierre Goloubinoff 4. Cell Stress Chaperones *10*, 329–339.

Marme, D., and A.J.Trewavas (1986). Molecular and Cellular Aspects of Calcium in Plant Developement (New York and London: Springer US).

Martinez, G.Q., and Gordon, S.E. (2019). Multimerization of Homo sapiens TRPA1 ion channel cytoplasmic domains. PLoS One *14*, 1–15.

Maser, P. (2001). Phylogenetic Relationships within Cation Transporter Families of Arabidopsis. Plant Physiol. *126*, 1646–1667.

Mccormack, E., Braam, J., and Braam, J. (2003). Calmodulins and related potential calcium sensors of Arabidopsis. 585–598.

Meena, M.K., and Vadassery, J. (2018). stress signaling Channels hold the key :

cyclic nucleotide gated channels (CNGC) in plant biotic stress signaling.

Meena, M.K., Prajapati, R., Krishna, D., Divakaran, K., Pandey, Y., Reichelt, M., Mathew, M.K., Boland, W., Mithöfer, A., and Vadassery, J. (2019). The Ca 2+ Channel CNGC19 Regulates Arabidopsis Defense Against Spodoptera Herbivory . Plant Cell *31*, 1539–1562.

Mithöfer, A., and Boland, W. (2012). Plant Defense Against Herbivores: Chemical Aspects. Annu. Rev. Plant Biol. *63*, 431–450.

Mousavi, S.A.R., Chauvin, A., Pascaud, F., Kellenberger, S., and Farmer, E.E. (2013). GLUTAMATE RECEPTOR-LIKE genes mediate leaf-to-leaf wound signalling. Nature *500*, 422–426.

Mühlberger, E. (2013). NIH Public Access. *2*, 205–215.

Murphy, G.J., and Isaacson, J.S. (2003). Presynaptic cyclic nucleotide-gated ion channels modulate neurotransmission in the mammalian olfactory bulb. Neuron *37*, 639–647.

Nawaz, Z., Kakar, K.U., Saand, M.A., and Shu, Q.Y. (2014). Cyclic nucleotide-gated ion channel gene family in rice, identification, characterization and experimental analysis of expression response to plant hormones, biotic and abiotic stresses. BMC Genomics *15*, 1–18.

Nejat, N., and Mantri, N. (2017). Plant immune system: Crosstalk between responses to biotic and abiotic stresses the missing link in understanding plant defence. Curr. Issues Mol. Biol. *23*, 1–16.

Orwick-Rydmark, M., Arnold, T., and Linke, D. (2016). The use of detergents to purify membrane proteins.

Pan, Y., Chai, X., Gao, Q., Zhou, L., Zhang, S., Li, L., and Luan, S. (2019). Dynamic Interactions of Plant CNGC Subunits and Calmodulins Drive Oscillatory Ca 2+ Channel Activities. Dev. Cell *48*, 710-725.e5.

Peiter, E. (2011). The plant vacuole: Emitter and receiver of calcium signals. Cell Calcium *50*, 120–128.

Penson, S.P., Schuurink, R.C., Fath, A., Gubler, F., John, V., Jones, R.L., Penson, S.P., Schuurink, R.C., Fath, A., Gubler, F., et al. (2016). cGMP Is Required for Gibberellic Acid-Induced Gene Expression in Barley Aleurone Linked references are available on JSTOR for this article : cGMP Is Required for Gibberellic Acid-Induced Gene Expression in Barley Aleurone. *8*, 2325–2333.

Rosano, G.L., and Ceccarelli, E.A. (2014). Recombinant protein expression in Escherichia coli: Advances and challenges. Front. Microbiol. *5*, 1–17.

Schuurink, R.C., Shartzer, S.F., Fath, A., and Jones, R.L. (1998). Characterization of a calmodulin-binding transporter from the plasma membrane of barley aleurone. Proc. Natl. Acad. Sci. U. S. A. *95*, 1944–1949.

Singha, I.M., Kakoty, Y., Unni, B.G., Kalita, M.C., Das, J., Naglot, A., Wann, S.B., and Singh, L. (2011). Secondary metabolites in plant defence mechanisms. World J. Microbiol. Biotechnol. *27*, 617–633.

Stoebel, D.M., Dean, A.M., and Dykhuizen, D.E. (2008). The cost of expression of Escherichia coli lac operon proteins is in the process, not in the products. Genetics *178*, 1653–1660.

Sunkar, R., Kaplan, B., Bouché, N., Arazi, T., Dolev, D., Talke, I.N., Maathuis, F.J.M., Sanders, D., Bouchez, D., and Fromm, H. (2000). Expression of a truncated tobacco NtCBP4 channel in transgenic plants and disruption of the homologous Arabidopsis CNGC1 gene confer Pb2+ tolerance. Plant J. *24*, 533–542.

Systems, S.T., Linder, M.B., Qiao, M., Laumen, F., Selber, K., and Hyytia, T. (2004). Efficient Purification of Recombinant Proteins Using Hydrophobins as Tags in. Biochemistry *43*, 11873–11882.

Talke, I.N., Blaudez, D., Maathuis, F.J.M., and Sanders, D. (2003). CNGCs: Prime targets of plant cyclic nucleotide signalling? Trends Plant Sci. *8*, 286–293.

Tunc-Ozdemir, M., Tang, C., Ishka, M.R., Brown, E., Groves, N.R., Myers, C.T., Rato, C., Poulsen, L.R., McDowell, S., Miller, G., et al. (2013a). A cyclic nucleotide-gated channel (CNGC16) in pollen is critical for stress tolerance in pollen reproductive development. Plant Physiol. *161*, 1010–1020.

Tunc-Ozdemir, M., Rato, C., Brown, E., Rogers, S., Mooneyham, A., Frietsch, S., Myers, C.T., Poulsen, L.R., Malhó, R., and Harper, J.F. (2013b). Cyclic Nucleotide Gated Channels 7 and 8 Are Essential for Male Reproductive Fertility. PLoS One *8*.

Tuteja, N., and Mahajan, S. (2007). Calcium signaling network in plants: An overview. Plant Signal. Behav. *2*, 79–85.

Vadassery, J., Reichelt, M., Hause, B., Gershenzon, J., Boland, W., and Mithöfer, A. (2012). CML42-mediated calcium signaling coordinates responses to Spodoptera herbivory and abiotic stresses in Arabidopsis. Plant Physiol. *159*, 1159–1175.

Vadassery, J., Ballhorn, D.J., Fleming, S.R., Mazars, C., Pandey, S.P., Schmidt, A., Schuman, M.C., Yeh, K.W., Yilamujiang, A., and Mithöfer, A. (2019). Neomycin: An Effective Inhibitor of Jasmonate-Induced Reactions in Plants. J. Plant Growth Regul. *38*, 713–722.

Vagenende, V., Yap, M.G.S., and Trout, B.L. (2009). Mechanisms of protein stabilization and prevention of protein aggregation by glycerol. Biochemistry *48*, 11084–11096.

War, A.R., Paulraj, M.G., Ahmad, T., Buhroo, A.A., Hussain, B., Ignacimuthu, S., and Sharma, H.C. (2012). Psb-7-1306. Plant Signal. Behav. *7*, 1306–1320.

Ward, J.M., Mäser, P., and Schroeder, J.I. (2009). Plant Ion Channels: Gene Families, Physiology, and Functional Genomics Analyses. Annu. Rev. Physiol. *71*, 59–82.

Widmann, M., Trodler, P., and Pleiss, J. (2010). The isoelectric region of proteins: A systematic analysis. PLoS One *5*.

Wu, J., and Baldwin, I.T. (2009). Herbivory-induced signalling in plants: Perception and action. Plant, Cell Environ. *32*, 1161–1174.

Yasui, K., Uegaki, M., Shiraki, K., and Ishimizu, T. (2010). Enhanced solubilization of membrane proteins by alkylamines and polyamines. Protein Sci. *19*, 486–493.

Yoshioka, K., Moeder, W., Kang, H.G., Kachroo, P., Masmoudi, K., Berkowitz, G., and Klessig, D.F. (2006). The chimeric Arabidopsis CYCLIC NUCLEOTIDE-GATED ION CHANNEL11/12 activates multiple pathogen resistance responses. Plant Cell *18*, 747–763.

Zhang, X., and Cote, R.H. (2005). cGMP signaling in vertebrate retinal photoreceptor cells. Front. Biosci. *10*, 1191–1204.

Zimmermann, M.R., Mithöfer, A., Will, T., Felle, H.H., and Furch, A.C.U. (2016). Herbivore-triggered electrophysiological reactions: Candidates for systemic signals in higher plants and the challenge of their identification. Plant Physiol. *170*, 2407–2419.